On stability of the evolution Galerkin schemes applied to a two-dimensional wave equation system[1]

M. Lukáčová-Medviďová,[2] G. Warnecke[3] and Y. Zahaykah[3]

Abstract

The subject of the paper is the analysis of stability of the evolution Galerkin (EG) methods for the two-dimensional wave equation system. We apply von Neumann analysis and use the Fourier transformation to estimate the stability limits of both the first and the second order EG methods.

Key words: hyperbolic systems, wave equation, evolution Galerkin schemes, discrete Fourier transformation, amplification matrix, CFL condition.

1 Introduction

Evolution Galerkin methods (EG-methods) were proposed to approximate first order hyperbolic problems. These schemes were introduced by Morton, see, e.g., [9] for scalar problems and [10] for one-dimensional systems. The first generalization to two-dimensional systems was made in [11] by Ostkamp for the wave equation system as well for the Euler equations of gas dynamics. In [4] Lukáčová, Morton and Warnecke systematically studied approximate evolution operators and constructed further EG-schemes with better accuracy and stability properties. Further EG schemes as well as the approximate evolution operator of the solution for the wave equation system in three space dimensions were derived in [13]. These methods or their finite volume versions were applied to the nonlinear Euler equations, see [1], [6], as well as to the linearized Euler equations and Maxwell equations [7]. Higher order finite volume EG-methods have been introduced and studied in [3], [5], [6] and [8].

The main objective of this paper is the analysis of the stability of the evolution Galerkin schemes. We derive a necessary and sufficient stability condition for the evolution Galerkin scheme (EG3 scheme) applied to the wave equation system in two space dimensions. The discrete Fourier transformation is used to obtain the amplification matrices of these schemes. Using estimates of the spectral norm we find a sufficient stability condition. We derive amplification matrices for the first and the second order finite volume schemes (FVEG) based on the approximate evolution operators. The spectral radius of the amplification matrices is estimated experimentally by a built-in Matlab procedure. Hence the stability limit of the schemes is estimated also numerically.

The outline of this paper is as follows: in the next section we survey the general theory that

[1]This research was supported by the VolkswagenStiftung Agency, by the Deutsche Forschungsgemeinschaft Grant No. Wa 633/6-2 and partially by the European network HYKE, funded by the EC as contract HPRN-CT-2002-00282. Authors gratefully acknowledge these supports.

[2]TU Hamburg-Harburg, Arbeitsbereich Mathematik, Schwarzenbergstrasse 95, 21073 Hamburg, Germany, email: lukacova@tu-harburg.de

[3]Institut für Analysis und Numerik, Otto-von-Guericke-Universität Magdeburg, Universitätsplatz 2, 39106 Magdeburg, Germany, emails: Gerald.Warnecke@mathematik.uni-magdeburg.de, Yousef.Zahaykah@mathematik.uni-magdeburg.de

we used to derive the exact integral equations. In Section 3 we recall the evolution Galerkin schemes. The exact integral equations as well as the approximate evolution operators for the two-dimensional wave equation system are given in Section 4. In Section 5 we introduce the discrete Fourier transformation as well as the spectral norm that serve as tools in our analysis. In Section 6 we present the derivation of the sufficient and necessary condition and compare the theoretical limit, that we obtained by means of the Fourier analysis with the experimental one. In Section 7 we consider the first order finite volume schemes based on the approximate evolution operator E_Δ^{const}. We determine the amplification matrices and estimate their stability limits. Finally in Section 8 we determine the amplification matrices of the second order finite volume schemes based on the approximate evolution operator E_Δ^{bilin} and estimate the stability limits.

2 General theory

In this section we recall the exact integral equations for a general linear hyperbolic system using the concept of bicharacteristics. Consider a general form of linear hyperbolic system

$$\mathbf{U}_t + \sum_{k=1}^{d} \mathcal{A}_k \mathbf{U}_{x_k} = 0, \;\; \mathbf{x} = (x_1, \ldots, x_d)^T \in \mathbb{R}^d, \tag{2.1}$$

where the coefficient matrices $\mathcal{A}_k, k = 1, ..., d$ are elements of $\mathbb{R}^{p\times p}$and the dependent variables are $\mathbf{U} = (u_1, ..., u_p)^T = \mathbf{U}(\mathbf{x}, t) \in \mathbb{R}^p$. Let $\mathcal{A}(\mathbf{n}) = \sum_{k=1}^d n_k \mathcal{A}_k$ be the **pencil matrix**, where $\mathbf{n} = (n_1, ..., n_d)^T$ is a unit vector in $\mathbb{R}^d$. Since the system (2.1) is hyperbolic the matrix $\mathcal{A}(\mathbf{n})$ has p real eigenvalues λ_k, $k = 1, ..., p$, and p corresponding linearly independent right eigenvectors $\mathbf{r}_k = \mathbf{r}_k(\mathbf{n})$, $k = 1, ..., p$. Let $\mathcal{R} = [\mathbf{r}_1|\mathbf{r}_2|...|\mathbf{r}_p]$ be the matrix of right eigenvectors. We define the characteristic variable $\mathbf{W} = \mathbf{W}(\mathbf{n})$ as $\partial\mathbf{W}(\mathbf{n}) = \mathcal{R}^{-1}\partial\mathbf{U}$. Since the system (2.1) has constant coefficient matrices $\mathcal{A}_k$ we have $\mathbf{W} = \mathcal{R}^{-1}\mathbf{U}$ or $\mathbf{U} = \mathcal{R}\,\mathbf{W}$.
Transforming system (2.1) by multiplying it with $\mathcal{R}^{-1}$ from the left we get

$$\mathcal{R}^{-1}\mathbf{U}_t + \sum_{k=1}^{d} \mathcal{R}^{-1}\mathcal{A}_k\mathcal{R}\,\mathcal{R}^{-1}\mathbf{U}_{x_k} = 0. \tag{2.2}$$

Let $\mathcal{B}_k = \mathcal{R}^{-1}\mathcal{A}_k\mathcal{R} = (b_{ij}^k)_{i,j=1}^p$, where $k = 1, 2, ..., d$, then the system (2.2) can be rewritten in the following form using characteristic variables

$$\mathbf{W}_t + \sum_{k=1}^{d} \mathcal{B}_k \mathbf{W}_{x_k} = 0.$$

Now we decompose $\mathcal{B}_k$ into the diagonal part $\mathcal{D}_k$ and the rest part $\mathcal{B}_k'$, i.e. $\mathcal{B}_k = \mathcal{D}_k + \mathcal{B}_k'$. We obtain

$$\mathbf{W}_t + \sum_{k=1}^{d} \mathcal{D}_k \mathbf{W}_{x_k} = -\sum_{k=1}^{d} \mathcal{B}_k' \mathbf{W}_{x_k} =: \mathbf{S}. \tag{2.3}$$

The i-th bicharacteristic corresponding to the i-th equation of (2.3) is defined by

$$\frac{d\mathbf{x}_i}{d\tilde{t}} = \mathbf{b}_{ii}(\mathbf{n}) = (b_{ii}^1, b_{ii}^2, ..., b_{ii}^d)^T,$$

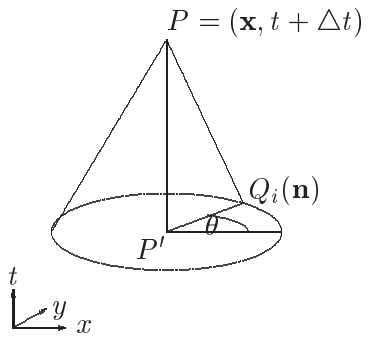

Figure 1: Bicharacteristics along the Mach cone through P and $Q_i(\mathbf{n})$, $d = 2$.

where $i = 1, ..., p$. The diagonal entries b_{ii}^k of the matrices $\mathcal{B}_k$, $k = 1, ..., d$, $i = 1, ..., p$, create the so-called ray velocity vector $\mathbf{b}_{ii}$. We consider the bicharacteristics backwards in time and set the initial conditions $\mathbf{x}_i(t + \Delta t, \mathbf{n}) = \mathbf{x}$ for all $\mathbf{n} \in \mathbb{R}^d$ and $i = 1, ..., p$, i.e. $\mathbf{x}_i(\tilde{t}, \mathbf{n}) = \mathbf{x} - \mathbf{b}_{ii}(\mathbf{n})(t + \Delta t - \tilde{t})$.
We will integrate the i-th equation of the system (2.3) from the point P down to the point $Q_i(\mathbf{n})$, where the bicharacteristic hits the plane at time t, see Figure 1. Note that bicharacteristics are straight lines because the system is linear having constant coefficients. Now the i-th equation reads

$$\frac{\partial w_i}{\partial t} + \sum_{k=1}^{d} b_{ii}^k \frac{\partial w_i}{\partial x_k} = -\left(\sum_{j=1, i \neq j}^{d} \left(b_{ij}^1 \frac{\partial w_j}{\partial x_1} + b_{ij}^2 \frac{\partial w_j}{\partial x_2} + ... + b_{ij}^d \frac{\partial w_j}{\partial x_d} \right) \right) = S_i, \tag{2.4}$$

where $P \equiv (\mathbf{x}, t + \Delta t) \in \mathbb{R}^p \times \mathbb{R}_+$ is taken to be a fixed point, while $Q_i(\mathbf{n}) = (\mathbf{x}_i(\mathbf{n}, t), t) = (\mathbf{x} - \Delta t \mathbf{b}_{ii}, t)$. Taking a vector $\sigma_i = (b_{ii}^1, b_{ii}^2, ..., b_{ii}^d, 1)$, we can define the directional derivative

$$\frac{dw_i}{d\sigma_i} = \left(\frac{\partial w_i}{\partial x_1}, \frac{\partial w_i}{\partial x_2}, ..., \frac{\partial w_i}{\partial x_d}, \frac{\partial w_i}{\partial t} \right) \cdot \sigma_i = \frac{\partial w_i}{\partial t} + b_{ii}^1 \frac{\partial w_i}{\partial x_1} + b_{ii}^2 \frac{\partial w_i}{\partial x_2} + ... + b_{ii}^d \frac{\partial w_i}{\partial x_d}.$$

Hence the i-th equation (2.4) can be rewritten as follows

$$\frac{dw_i}{d\sigma_i} = S_i = -\sum_{j=1, i \neq j}^{d} \left(b_{ij}^1 \frac{\partial w_j}{\partial x_1} + b_{ij}^2 \frac{\partial w_j}{\partial x_2} + ... + b_{ij}^d \frac{\partial w_j}{\partial x_d} \right).$$

Integration from P to $Q_i(\mathbf{n})$ gives

$$w_i(P) - w_i(Q_i(\mathbf{n})) = S_i', \tag{2.5}$$

where

$$S_i' = \int_t^{t+\Delta t} S_i(\mathbf{x}_i(\tilde{t}, \mathbf{n}), \tilde{t}, \mathbf{n}) d\tilde{t} = \int_0^{\Delta t} S_i(\mathbf{x}_i(\tau, \mathbf{n}), t + \Delta t - \tau, \mathbf{n}) \mathrm{d}\tau.$$

Reverse transformation of (2.5) into the system written in original physical variables is done by multiplication with $\mathcal{R}$ from the left and $(d-1)-$dimensional integration of the variable

$\mathbf{n}$ over the unit sphere O in $\mathbb{R}^d$. This leads to the integral representation of the solution at point at time $t + \Delta t$

$$\mathbf{U}(P) = \mathbf{U}(\mathbf{x}, t + \Delta t) = \frac{1}{|O|} \int_O \mathcal{R}(\mathbf{n}) \begin{pmatrix} w_1(Q_1(\mathbf{n}), \mathbf{n}) \\ w_2(Q_2(\mathbf{n}), \mathbf{n}) \\ w_3(Q_3(\mathbf{n}), \mathbf{n}) \\ \vdots \\ w_p(Q_p(\mathbf{n}), \mathbf{n}) \end{pmatrix} \mathrm{d}O + \tilde{\mathbf{S}}, \tag{2.6}$$

where

$$\tilde{\mathbf{S}} = (\tilde{S}_1, \tilde{S}_2, ..., \tilde{S}_p)^T = \frac{1}{|O|} \int_O \mathcal{R}(\mathbf{n}) \mathbf{S}' \mathrm{d}O = \frac{1}{|O|} \int_O \int_0^{\Delta t} \mathcal{R}(\mathbf{n}) \mathbf{S}(t + \Delta t - \tau, \mathbf{n}) \mathrm{d}\tau \mathrm{d}O$$

and $|O|$ corresponds to the measure of the domain of integration.

3 Exact integral equations and approximate evolution operators for the wave equation system

In this section we illustrate the application of general theory of the bicharacteristics for the two-dimensional system of wave equation. We recall the exact integral equations and present their possible approximation, the so-called EG3 approximate evolution operator. Consider the two dimensional wave equation system

$$\begin{aligned} \phi_t + c(u_x + v_y) &= 0, \\ u_t + c\phi_x &= 0, \\ v_t + c\phi_y &= 0, \end{aligned} \tag{3.1}$$

where c is a given constant representing the speed of sound. We will recall here the exact integral equations derived in [4]. Let $P = (x, y, t + \Delta t)$, $P' = (x, y, t)$, $Q = (x + c\Delta t \cos\theta, y + c\Delta t \sin\theta, t) = (\mathbf{x} + c\Delta t \mathbf{n}(\theta), t)$ and the so-called source term be given as

$$S = c\left[u_x \sin^2\theta - (u_y + v_x)\sin\theta\cos\theta + v_y \cos^2\theta\right], \tag{3.2}$$

then **exact integral equations** for the wave equation system (3.1) are given as

$$\phi_P = \frac{1}{2\pi} \int_0^{2\pi} (\phi_Q - u_Q \cos\theta - v_Q \sin\theta)\, d\theta + \tilde{S}_1, \tag{3.3}$$

$$u_P = \frac{1}{2} u_{P'} + \frac{1}{2\pi} \int_0^{2\pi} (-\phi_Q \cos\theta + u_Q \cos^2\theta + v_Q \sin\theta \cos\theta)\, d\theta + \tilde{S}_2, \tag{3.4}$$

$$v_P = \frac{1}{2} v_{P'} + \frac{1}{2\pi} \int_0^{2\pi} (-\phi_Q \sin\theta + u_Q \cos\theta \sin\theta + v_Q \sin^2\theta\, d\theta + \tilde{S}_3, \tag{3.5}$$

where

$$\tilde{S}_1 = \frac{-1}{2\pi}\int_0^{2\pi}\int_0^{\triangle t} S(\mathbf{x}+c\tau\mathbf{n}(\theta), t+\Delta t-\tau, \theta)\,\mathrm{d}\tau\,\mathrm{d}\theta,$$

$$\tilde{S}_2 = \frac{1}{2\pi}\int_0^{2\pi}\int_0^{\triangle t} \cos\theta S(\mathbf{x}+c\tau\mathbf{n}(\theta), t+\Delta t-\tau, \theta)\,\mathrm{d}\tau\,\mathrm{d}\theta$$

$$-\frac{1}{2\pi}\int_0^{2\pi}\int_0^{\triangle t} \left[c\phi_x(\mathbf{x}, t+\Delta t-\tau)\sin^2\theta - c\phi_y(\mathbf{x}, t+\Delta t-\tau)\sin\theta\cos\theta\right]\,\mathrm{d}\tau\,\mathrm{d}\theta,$$

$$\tilde{S}_3 = \frac{1}{2\pi}\int_0^{2\pi}\int_0^{\triangle t} \sin\theta S(\mathbf{x}+c\tau\mathbf{n}(\theta), t+\Delta t-\tau, \theta)\,\mathrm{d}\tau\,\mathrm{d}\theta$$

$$-\frac{1}{2\pi}\int_0^{2\pi}\int_0^{\triangle t} \left[c\phi_y(\mathbf{x}, t+\Delta t-\tau)\cos^2\theta - c\phi_x(\mathbf{x}, t+\Delta t-\tau)\sin\theta\cos\theta\right]\,\mathrm{d}\tau\,\mathrm{d}\theta.$$

The above integral equations give us an implicit formulation of the solution at the point $P = (x, y, t^{n+1})$. In order to obtain an explicit numerical scheme it is necessary to use some numerical quadratures in order to approximate the time integral from 0 to Δt. Using the backward rectangle rule leads to an $\mathcal{O}(\Delta t^2)$ approximation of the time integrals appearing in $\tilde{S}_1$, $\tilde{S}_2$ and $\tilde{S}_3$. Further we use the following result [4, Lemma 2.1]

$$\begin{aligned}
\Delta t\int_0^{2\pi} S(t,\theta)\mathrm{d}\theta &= \int_0^{2\pi}(u\cos\theta + v\sin\theta)\mathrm{d}\theta,\\
\Delta t\int_0^{2\pi} S(t,\theta)\cos\theta\mathrm{d}\theta &= \int_0^{2\pi}(u\cos 2\theta + v\sin 2\theta)\mathrm{d}\theta,\\
\Delta t\int_0^{2\pi} S(t,\theta)\sin\theta\mathrm{d}\theta &= \int_0^{2\pi}(u\sin 2\theta + v\cos 2\theta)\mathrm{d}\theta. \qquad (3.6)
\end{aligned}$$

Note that these formulae allow to replace the derivatives of our dependent variables in S by the variables themselves. Rectangle rule approximation for the time integral and (3.6) yield the so-called EG3 approximate evolution operator. We refer a reader to [4], [13] for other approximate evolution operators EG1-EG4.

Approximate evolution operator for EG3

$$\phi_P = \frac{1}{2\pi}\int_0^{2\pi}(\phi_Q - 2u_Q\cos\theta - 2v_Q\sin\theta)\mathrm{d}\theta + O(\Delta t^2) \qquad (3.7)$$

$$u_P = \frac{1}{2}u_{P'} + \frac{1}{2\pi}\int_0^{2\pi}(-2\phi_Q\cos\theta + (3\cos^2\theta - 1)u_Q\cos^2\theta + 3v_Q\sin\theta\cos\theta)\mathrm{d}\theta + O(\Delta t^2) \qquad (3.8)$$

$$v_P = \frac{1}{2}v_{P'} + \frac{1}{2\pi}\int_0^{2\pi}(-2\phi_Q\sin\theta + 3u_Q\sin\theta\cos\theta + (3\sin^2\theta - 1)v_Q\sin^2\theta)\mathrm{d}\theta + O(\Delta t^2). \qquad (3.9)$$

4 Evolution Galerkin Schemes

In this section we describe the evolution Galerkin schemes in the finite difference framework as well as the finite volume evolution Galerkin schemes. The main idea of the evolution Galerkin schemes is the following. Transported quantities are shifted along the bicharacteristics and then projected onto a finite element space. These methods connect the finite element ideas with the theory of bicharacteristics. In the finite volume framework the approximate operators are used only in order to compute fluxes on cell interfaces. Thus, instead of the one-dimensional Riemann solvers, which work only in the normal directions to the cell interfaces, we compute the approximate solution at cell interfaces by a multi-dimensional evolution operator. This can be considered as a predictor step. In the corrector step the finite volume update is made.
Consider a mesh in $\mathbb{R}^2$, which consists of the square mesh cells

$$\Omega_{kl} = \left[(k-\frac{1}{2})h, (k+\frac{1}{2})h\right] \times \left[(l-\frac{1}{2})h, (l+\frac{1}{2})h\right] = \left[x_k - \frac{h}{2}, x_k + \frac{h}{2}\right] \times \left[y_l - \frac{h}{2}, y_l + \frac{h}{2}\right],$$

where, $h > 0$ is the mesh size parameter, $k, l \in \mathbb{Z}$. Let us denote by $H^\kappa(\mathbb{R}^2)$ the Sobolev space of distributions with derivatives up to the order κ in L^2 space, where $\kappa \in \mathbb{N}$. Consider the general hyperbolic system given by the equation (2.1). Let us denote by $E(s) : (H^\kappa(\mathbb{R}^2))^p \to (H^\kappa(\mathbb{R}^2))^p$ the exact evolution operator for the system (2.1), i.e.

$$\mathbf{U}(., t+s) = E(s)\mathbf{U}(., t). \tag{4.1}$$

We suppose that S_h^m is a finite element space consisting of piecewise polynomials of order $m \geq 0$ with respect to the square mesh. Assume a constant time step, i.e. $t_n = n\Delta t$. Let $\mathbf{U}^n$ be an approximation in the space S_h^m to the exact solution $\mathbf{U}(., t_n)$ at time $t_n \geq 0$. We consider $E_\tau : (L^1_{loc}(\mathbb{R}^2))^p \to (H^\kappa(\mathbb{R}^2))^p$ to be a suitable approximate evolution operator for $E(\tau)$. In practice we will use restrictions of E_τ to the subspace S_h^m for $m \geq 0$. Then we can define the general class of evolution Galerkin methods.

Definition 4.2 *Starting from some initial data $\mathbf{U}^0 \in S_h^m$ at time $t = 0$, an evolution Galerkin method (EG-method) is recursively defined by means of*

$$\mathbf{U}^{n+1} = P_h E_\tau \mathbf{U}^n, \tag{4.3}$$

where P_h is the L^2-projection given by the integral averages in the following way

$$P_h \mathbf{U}^n|_{\Omega_{kl}} = \frac{1}{|\Omega_{kl}|} \int_{\Omega_{kl}} \mathbf{U}(x, y, t_n)\, dxdy. \tag{4.4}$$

We denote by $R_h : S_h^m \to S_h^r$ a recovery operator, $r > m \geq 0$ and consider our approximate evolution operator E_τ on S_h^r. In this paper we will limit our considerations to the cases where $m = 0$. In this case the integrals that we obtained from the projection are evaluated either exactly using the fact that the approximate values $\mathbf{U}^n$ are piecewise constants or by means of some numerical quadratures. Using piecewise constants the resulting schemes will only be of first order, even when E_τ is approximated to a higher order. Higher order accuracy can be obtained either by taking $m > 0$, or by inserting a recovery stage R_h before the evolution step in equation (4.3) to give

$$\mathbf{U}^{n+1} = P_h E_\tau R_h \mathbf{U}^n. \tag{4.5}$$

To implement (4.5) rather complex three-dimensional integrals need to be evaluated exactly. This approach seemed to be hardly feasible for effective derivation and implementation of higher order methods. A simplification that we used was the application of the multidimensional evolution only on the cell interfaces. This leads to the finite volume evolution Galerkin methods.

Definition 4.6 *Starting from some initial data* $\mathbf{U}^0 \in S_h^m$*, the finite volume evolution Galerkin method (FVEG) is recursively defined by means of*

$$\mathbf{U}^{n+1} = \mathbf{U}^n - \frac{1}{h}\int_0^{\Delta t} \sum_{j=1}^{2} \delta_{x_j} \mathbf{f}_j(\tilde{\mathbf{U}}^{n+\frac{\tau}{\Delta t}})\, d\tau, \tag{4.7}$$

where $\delta_{x_j}\mathbf{f}_j(\tilde{\mathbf{U}}^{n+\frac{\tau}{\Delta t}})$ *represents an approximation to the edge flux difference and* δ_x *is defined by* $\delta_x v(x) = v(x+\frac{h}{2}) - v(x-\frac{h}{2})$*. The cell boundary value* $\tilde{\mathbf{U}}^{n+\frac{\tau}{\Delta t}}$ *is evolved using the approximate evolution operator* E_τ *to* $t_n + \tau$ *and averaged a long the cell boundary, i.e.*

$$\tilde{\mathbf{U}}^{n+\frac{\tau}{\Delta t}} = \sum_{k,l\in\mathbb{Z}} \left(\frac{1}{|\partial\Omega_{kl}|} \int_{\partial\Omega_{kl}} E_\tau R_h \mathbf{U}^n dS \right) \chi_{kl}, \tag{4.8}$$

where χ_{kl} *is the characteristic function of* $\partial\Omega_{kl}$*.*

For more details on the higher order finite volume evolution Galerkin (FVEG) schemes, see [1], [6], [8], where the error analysis as well as numerical experiments are presented. Using the L^2-projection (4.4), the approximate evolution operator E_τ, and (4.7), (4.8) the finite difference formulae for both the EG and the FVEG schemes can be written in the form

$$\mathbf{U}_{kl}^{n+1} = \mathbf{U}_{kl}^n + \sum_{r=1-}^{1} \sum_{s=-1}^{1} \mathcal{C}_{rs} \mathbf{U}_{k+rl+s}^n, \tag{4.9}$$

where

$$\mathcal{C}_{rs} = \begin{pmatrix} \alpha_{rs}^1 & \beta_{rs}^1 & \gamma_{rs}^1 \\ \alpha_{rs}^2 & \beta_{rs}^2 & \gamma_{rs}^2 \\ \alpha_{rs}^3 & \beta_{rs}^3 & \gamma_{rs}^3 \end{pmatrix}. \tag{4.10}$$

Here the entries $\alpha_{rs}^m, \beta_{rs}^m, \gamma_{rs}^m$, $m = 1,2,3$ are taken appropriately according to the approximate evolution operator E_τ used. In the Appendix the stencil matrices α^m, β^m and γ^m, $m = 1,2,3$ are written for some EG schemes.

5 Basic tools

As we mentioned above our stability considerations are based on Fourier analysis. We first recall some basic concepts. Let $\{\psi_{kl}^n\}_{k,l=-\infty}^{\infty}$ be a two dimensional sequence in ℓ_2.

Definition 5.1 *The discrete Fourier transformation of* $\{\psi_{kl}^n\} \in \ell_2$ *is the function* $\hat{\psi}^n \in L_2\left(\left[-\frac{\pi}{h}, \frac{\pi}{h}\right]^2\right)$ *defined by*

$$\hat{\psi}^n = h^2 \sum_{k=-\infty}^{\infty} \sum_{l=-\infty}^{\infty} \psi_{kl}^n \exp^{-ih(k\xi+l\eta)}.$$

Similar to the case of continuous Fourier transformation, there are both an inversion formula and Parseval's equality.

Lemma 5.2 *(Inverse formula) If* $\{\psi_{kl}^n\} \in \ell_2$ *and* $\hat{\psi^n}$ *is the discrete Fourier transformation of* $\{\psi_{kl}^n\}$*, then*

$$\psi_{kl}^n = \frac{1}{4\pi^2} \int_{-\frac{\pi}{h}}^{\frac{\pi}{h}} \int_{-\frac{\pi}{h}}^{\frac{\pi}{h}} \hat{\psi^n} \exp^{ih(k\xi+l\eta)} \, d\xi \, d\eta.$$

Lemma 5.3 *(Parseval's equality) If* $\{\psi_{kl}^n\} \in \ell_2$ *and* $\hat{\psi^n}$ *is the discrete Fourier transformation of* $\{\psi_{kl}^n\}$*, then*

$$||\hat{\psi^n}|| = ||\psi_{kl}^n||,$$

where the first norm is the L_2*-norm on* $\left[-\frac{\pi}{h}, \frac{\pi}{h}\right] \times \left[-\frac{\pi}{h}, \frac{\pi}{h}\right]$ *and the second norm is the* ℓ_2*-norm.*

Hence we have the following result.

Lemma 5.4 *The sequence* $\{\psi_{kl}^n\}$ *is bounded in* ℓ_2 *if and only if the sequence* $\{\hat{\psi^n}\}$ *is bounded in* $L_2\left(\left[-\frac{\pi}{h}, \frac{\pi}{h}\right] \times \left[-\frac{\pi}{h}, \frac{\pi}{h}\right]\right)$.

In order to study the stability of linear numerical schemes the Fourier transformation is used. This leads to the estimation of the spectral radius of the so-called amplification matrix. The spectral radius of a square complex matrix $\mathcal{A}$ with eigenvalues λ_i is defined to be

$$\rho(\mathcal{A}) = \max_i |\lambda_i|. \tag{5.5}$$

The spectral norm of the matrix $\mathcal{A}$ is defined as

$$||\mathcal{A}|| = \sup_{\mathbf{x} \neq 0} \frac{||\mathcal{A}\mathbf{x}||}{||\mathbf{x}||}. \tag{5.6}$$

The norms on the right hand side of equation (5.6) are the Euclidean norms of the vectors $\mathcal{A}\mathbf{x}$ and $\mathbf{x}$, respectively. Note that for the spectral norm, as for any matrix norm, we always have $||\mathcal{A}|| \geq \rho(\mathcal{A})$.

6 Estimate of the stability limit

In [4, Lemma 5.1] Lukáčová *et al.* proved the following stability result for the EG-schemes. There exists $\nu_{max} < 1$ such that the EG schemes for the two-dimensional wave equation system (3.1) are stable for any ν such that $0 \leq \nu \leq \nu_{max}$, where $\nu = c\frac{\Delta t}{h}$ is the CFL number. The goal of this section is to estimate precisely ν_{max} for the EG3 scheme. Analogous calculations can be done also for other EG-schemes of type EG1-EG4 as well as for the FVEG schemes. We apply the discrete Fourier transformation on both sides of equation (4.9).

$$\hat{\mathbf{U}}^{n+1} = \hat{\mathbf{U}}^n + h^2 \sum_{k=-\infty}^{\infty} \sum_{l=-\infty}^{\infty} \left(\sum_{r=-1}^{1} \sum_{s=-1}^{1} \mathcal{C}_{rs} \mathbf{U}_{k+rl+s}^n \right) \exp^{-ih(k\xi+l\eta)}. \tag{6.1}$$

By making the change of variables $k' = k + r$ and $l' = l + s$ we get

$$
\begin{aligned}
h^2 \sum_{k=-\infty}^{\infty} \sum_{l=-\infty}^{\infty} \left(\sum_{r=-1}^{1} \sum_{s=-1}^{1} \mathcal{C}_{rs} \mathbf{U}^n_{k+rl+s} \right) \exp^{-ih(k\xi+l\eta)} \\
&= \sum_{r=-1}^{1} \sum_{s=-1}^{1} \mathcal{C}_{rs} \exp^{ih(r\xi+s\eta)} \left(h^2 \sum_{k'=-\infty}^{\infty} \sum_{l'=-\infty}^{\infty} \mathbf{U}^n_{k'l'} \exp^{-ih(k'\xi+l'\eta)} \right) \\
&= \sum_{r=-1}^{1} \sum_{s=-1}^{1} \mathcal{C}_{rs} \exp^{ih(r\xi+s\eta)} \hat{\mathbf{U}}^n \qquad (6.2)
\end{aligned}
$$

Thus using this expression in the equation (6.1) we get

$$
\hat{\mathbf{U}}^{n+1} = \left(\mathcal{I} + \sum_{r=-1}^{1} \sum_{s=-1}^{1} \mathcal{C}_{rs} \exp^{ih(r\xi+s\eta)} \right) \hat{\mathbf{U}}^n, \qquad (6.3)
$$

where $\mathcal{I}$ is the identity matrix. The coefficient of $\hat{\mathbf{U}}^n$ in the equation (6.3),

$$
\mathcal{T}(\xi, \eta) = \mathcal{I} + \sum_{r=-1}^{1} \sum_{s=-1}^{1} \mathcal{C}_{rs} \exp^{ih(r\xi+s\eta)}, \qquad (6.4)
$$

is called the amplification matrix of the finite difference scheme (4.9). Applying recursively the result of equation (6.3) $n+1$ times yields

$$
\hat{\mathbf{U}}^{n+1} = \left(\mathcal{I} + \sum_{r=-1}^{1} \sum_{s=-1}^{1} \mathcal{C}_{rs} \exp^{ih(r\xi+s\eta)} \right)^{n+1} \hat{\mathbf{U}}^0 = \mathcal{T}^{n+1}(\xi, \eta) \hat{\mathbf{U}}^0. \qquad (6.5)
$$

We note that if $||\mathcal{T}(\xi, \eta)|| \leq 1$ then $||\hat{\mathbf{u}}^{n+1}|| \leq ||\hat{\mathbf{u}}^0||$, which means that the $\{\hat{\mathbf{u}}^n\}$ is L^2-stable. Consider the EG3 scheme, i.e. the numerical scheme based on equations (3.7) - (3.9), cf. also stencil matrices in the Appendix. After some calculation we obtain the following entries of the amplification matrix $\mathcal{T}(\xi, \eta)$

$$
\begin{aligned}
T_{11}(\xi, \eta) &= 1 + \frac{\nu^2}{\pi} - \frac{4\nu}{\pi} + \frac{\nu^2}{\pi} \cos(h\xi) \cos(h\eta) + \left(\frac{2\nu}{\pi} - \frac{\nu^2}{\pi} \right) (\cos(h\xi) + \cos(h\eta)), \\
T_{12}(\xi, \eta) &= -i \left(\frac{4\nu^2}{3\pi} \sin(h\xi) \cos(h\eta) + \left(\nu - \frac{4\nu^2}{3\pi} \right) \sin(h\xi) \right), \\
T_{13}(\xi, \eta) &= -i \left(\frac{4\nu^2}{3\pi} \cos(h\xi) \sin(h\eta) + \left(\nu - \frac{4\nu^2}{3\pi} \right) \sin(h\eta) \right), \\
T_{22}(\xi, \eta) &= 1 - \frac{2\nu}{\pi} + \frac{\nu^2}{2\pi} + \frac{\nu^2}{2\pi} \cos(h\xi) \cos(h\eta) + \left(\frac{2\nu}{\pi} - \frac{\nu^2}{2\pi} \right) \cos(h\xi) - \frac{\nu^2}{2\pi} \cos(h\eta), \\
T_{23}(\xi, \eta) &= \frac{-3\nu^2}{8} \sin(h\xi) \sin(h\eta), \\
T_{33}(\xi, \eta) &= 1 - \frac{2\nu}{\pi} + \frac{\nu^2}{2\pi} + \frac{\nu^2}{2\pi} \cos(h\xi) \cos(h\eta) + \left(\frac{2\nu}{\pi} - \frac{\nu^2}{2\pi} \right) \cos(h\eta) - \frac{\nu^2}{2\pi} \cos(h\xi), \\
T_{21}(\xi, \eta) &= T_{12}(\xi, \eta), \qquad T_{31}(\xi, \eta) = T_{13}(\xi, \eta), \qquad T_{32}(\xi, \eta) = T_{23}(\xi, \eta).
\end{aligned}
$$

Using the substitutions $S_\xi = \sin(h\xi)$, $s_\xi = \sin(\frac{h\xi}{2})$, $S_\eta = \sin(h\eta)$ and $s_\eta = \sin(\frac{h\eta}{2})$ the amplification matrix $\mathcal{T} = \mathcal{T}(\xi, \eta)$ can be written as

$$\mathcal{T} = \begin{pmatrix} C_{11} & -i\nu C_\xi & -i\nu C_\eta \\ i\nu C_\xi & C_{22} & \nu^2 C_{\xi\eta} \\ i\nu C_\eta & \nu^2 C_{\xi\eta} & C_{33} \end{pmatrix},$$

where

$$\begin{aligned} C_{11} &= 1 - \frac{4\nu}{\pi}(s_\xi^2 + s_\eta^2) + \frac{4\nu^2}{\pi} s_\xi^2 s_\eta^2, \\ C_\xi &= S_\xi(1 - \frac{8\nu}{3\pi} s_\eta^2), \\ C_\eta &= S_\eta(1 - \frac{8\nu}{3\pi} s_\xi^2), \\ C_{\xi\eta} &= \frac{-3}{8} S_\xi S_\eta, \\ C_{22} &= 1 - \frac{4\nu}{\pi} s_\xi^2 + \frac{2\nu^2}{\pi} s_\xi^2 s_\eta^2, \\ C_{33} &= 1 - \frac{4\nu}{\pi} s_\eta^2 + \frac{2\nu^2}{\pi} s_\xi^2 s_\eta^2. \end{aligned}$$

Set $\mathcal{E} = \begin{pmatrix} i & 0 & 0 \\ 0 & 1 & 0 \\ 0 & 0 & 1 \end{pmatrix}$, then $\mathcal{Q} = \begin{pmatrix} C_{11} & \nu C_\xi & \nu C_\eta \\ -\nu C_\xi & C_{22} & \nu^2 C_{\xi\eta} \\ -\nu C_\eta & \nu^2 C_{\xi\eta} & C_{33} \end{pmatrix} = \mathcal{E}^{-1}\mathcal{T}\mathcal{E}$, which means that $\mathcal{T}$ and $\mathcal{Q}$ are similar matrices and thus they have the same eigenvalues. Moreover, the matrix $\mathcal{Q}$ can be decomposed as

$$\mathcal{Q} = \mathcal{I} - \nu\,(\mathcal{D} + \mathcal{C}) + \nu^2 \tilde{\mathcal{C}},$$

where

$$\begin{aligned} \mathcal{D} &= \begin{pmatrix} d+f & 0 & 0 \\ 0 & d & 0 \\ 0 & 0 & f \end{pmatrix}, \quad \mathcal{C} = \begin{pmatrix} 0 & C_\xi & C_\eta \\ -C_\xi & 0 & 0 \\ -C_\eta & 0 & 0 \end{pmatrix}, \quad \tilde{\mathcal{C}} = \begin{pmatrix} 0 & 0 & 0 \\ 0 & 0 & C_{\xi\eta} \\ 0 & C_{\xi\eta} & 0 \end{pmatrix}, \\ d &= \frac{4}{\pi} s_\xi^2 - \frac{2\nu}{\pi} s_\xi^2 s_\eta^2 = \frac{2}{\pi} s_\xi^2 (2 - \nu s_\eta^2), \quad f = \frac{4}{\pi} s_\eta^2 - \frac{2\nu}{\pi} s_\xi^2 s_\eta^2 = \frac{2}{\pi} s_\eta^2 (2 - \nu s_\xi^2). \end{aligned}$$

Since

$$||\,\mathcal{Q} - (\mathcal{I} - \nu(\mathcal{D} + \mathcal{C}))|| \le \nu^2 |C_{\xi\eta}| \le \frac{3\nu^2}{8} = \mathcal{O}(\nu^2). \tag{6.6}$$

we can approximate the eigenvalues of $\mathcal{Q}$ by the eigenvalues of $\mathcal{H} = \mathcal{I} - \nu(\mathcal{D} + \mathcal{C})$ with the $\mathcal{O}(\nu^2)$ error. Note that for all $[\xi,\, \eta] \in [\frac{-\pi}{h}, \frac{\pi}{h}] \times [\frac{-\pi}{h}, \frac{\pi}{h}]$ the entries of $\mathcal{H}$ are bounded. To estimate the stability limit of the EG3 scheme we need to estimate spectral radius of $\mathcal{Q}$ for all choices of ξ, η and ν, $0 \le \nu \le 1$. Since $0 \le s_\xi^2 \le 1$ and $0 \le s_\eta^2 \le 1$ and $\nu \le 1$ then $d \ge 0$ and $f \ge 0$. Now the matrices $\mathcal{D}$, $\mathcal{C}$ are real and $\mathcal{C}$ is antisymmetric as well. Hence $\mathcal{D} + \mathcal{C}$ has either three real eigenvalues or one real eigenvalue and two complex conjugate eigenvalues.

Consider a *real eigenvalue*, say $\lambda = \lambda_r$. Let $\mathbf{v} = (v_1, v_2, v_3)$ be the corresponding eigenvector, then $\mathbf{v}^T(\mathcal{D} + \mathcal{C})\mathbf{v} = \mathbf{v}^T \lambda_r \mathbf{v}$. Since $\mathcal{C}$ is antisymmetric then $\mathbf{v}^T \mathcal{C} \mathbf{v} = 0$. Hence we get

$$(d + f - \lambda_r)v_1^2 + (d - \lambda_r)v_2^2 + (f - \lambda_r)v_3^2 = 0. \tag{6.7}$$

Since the coefficients in equation (6.7) can not have all the same sign, we get the estimates

$$0 \leq \min(d, f) \leq \lambda_r \leq d + f. \tag{6.8}$$

Let μ_r be a real eigenvalue of $\mathcal{H}$ then $\mu_r = 1 - \nu\lambda_r$. Hence $|\mu_r| \leq 1$ is equivalent to $-1 \leq 1 - \nu\lambda_r \leq 1$. Using inequality (6.8) we get

$$1 - \frac{4\nu}{\pi}\left(s_\xi^2 + s_\eta^2\right) + \frac{4\nu^2}{\pi} s_\xi^2 s_\eta^2 \leq 1 - \nu\lambda_r \leq 1.$$

To get $|\mu_r| \leq 1$ we need

$$1 - \frac{4\nu}{\pi}\left(s_\xi^2 + s_\eta^2\right) + \frac{4\nu^2}{\pi} s_\xi^2 s_\eta^2 \geq -1.$$

The last inequality reads

$$\nu^2\left(\frac{4}{\pi} s_\xi^2 s_\eta^2\right) - \nu\left(\frac{4}{\pi}\left(s_\xi^2 + s_\eta^2\right)\right) + 2 \geq 0. \tag{6.9}$$

Now, we want to bound ν such that $2 - \nu\frac{4}{\pi}\left(s_\xi^2 + s_\eta^2\right) \geq 0$. Hence inequality (6.9) yields

$$\begin{aligned} \nu^2\left(\frac{4}{\pi} s_\xi^2 s_\eta^2\right) - \nu\left(\frac{4}{\pi}\left(s_\xi^2 + s_\eta^2\right)\right) + 2 &\geq 2 - \frac{4\nu}{\pi}\left(s_\xi^2 + s_\eta^2\right) \\ &\geq 2 - \frac{8\nu}{\pi} \geq 0. \end{aligned}$$

The last inequality gives

$$\nu \leq \frac{\pi}{4} \approx 0.7854. \tag{6.10}$$

Now let us assume that μ_c is a *complex eigenvalue* of $\mathcal{H}$. Then $\mu_c = 1 - \nu\lambda_c$, where $\nu\lambda_c$ is a complex eigenvalue of the matrix $\mathcal{D} + \mathcal{C}$. This implies

$$|\mu_c|^2 = 1 - 2\nu Re(\lambda_c) + \nu^2|\lambda_c|^2.$$

Thus $|\mu_c|^2 \leq 1$ is equivalent to $\nu^2|\lambda_c|^2 - 2\nu Re(\lambda_c) \leq 0$. Suppose that $\lambda_r > 0$ then

$$\nu^2\lambda_r|\lambda_c|^2 - 2\nu\lambda_r Re(\lambda_c) \leq 0. \tag{6.11}$$

Let $b = C_\xi$ and $c = C_\eta$. It is well known that

$$\begin{aligned} det(\mathcal{D} + \mathcal{C}) &= d^2 f + f^2 d + b^2 f + c^2 d = \lambda_r|\lambda_c|^2, \\ Tr(\mathcal{D} + \mathcal{C}) &= 2(d + f) = \lambda_r + \lambda_c + \bar{\lambda_c} = \lambda_r + 2Re(\lambda_c), \end{aligned}$$

Hence inequality (6.11) reads

$$p(\lambda_r) = \lambda_r^2 - 2(d + f)\lambda_r + \nu(d^2 f + f^2 d + b^2 f + c^2 d) \leq 0. \tag{6.12}$$

The discriminant Δ of p gives

$$\Delta^2 = 4(d + f)^2 - 4\nu(d^2 f + f^2 d + b^2 f + c^2 d) = 4(d^2 + f^2) + 8fd - 4\nu(d^2 f + f^2 d + b^2 f + c^2 d).$$

We will assume that

$$8fd - 4\nu(d^2 f + f^2 d + b^2 f + c^2 d) \geq 0,$$

which leads to $\Delta^2 \geq 4(d^2 + f^2) \geq 0$ and we obtain

$$\begin{aligned} 8fd = \frac{32}{\pi^2} s_\xi^2 s_\eta^2 (2 - \nu s_\eta^2)(2 - \nu s_\xi^2) &= \frac{32}{\pi^2} s_\xi^2 s_\eta^2 (4 - 2\nu(s_\xi^2 + s_\eta^2) + \nu^2 s_\xi^2 s_\eta^2) \\ &\geq \frac{32}{\pi^2} s_\xi^2 s_\eta^2 (4 - 2\nu(s_\xi^2 + s_\eta^2)). \end{aligned}$$

Hence,

$$8fd \geq \frac{32}{\pi^2} s_\xi^2 s_\eta^2 (4 - 4\nu) = \frac{128}{\pi^2} s_\xi^2 s_\eta^2 (1 - \nu). \tag{6.13}$$

Further we have

$$\begin{aligned} d^2 f &= \frac{8}{\pi^3} s_\xi^2 s_\eta^2 (2 - \nu s_\eta^2)^2 (2 - \nu s_\xi^2) \leq \frac{64}{\pi^3} s_\xi^2 s_\eta^2 \leq \frac{64}{\pi^3}, \\ b^2 f &= S_\xi^2 (1 - \frac{8\nu^2}{3\pi} s_\eta^2)^2 \frac{2}{\pi} s_\eta^2 (2 - \nu s_\xi^2) \leq \frac{4}{\pi} S_\xi^2 s_\eta^2 \leq \frac{4}{\pi}. \end{aligned}$$

Analogously, we obtain

$$f^2 d \leq \frac{64}{\pi^3} \qquad \text{and} \qquad c^2 d \leq \frac{4}{\pi}.$$

Therefore,

$$-4\nu(d^2 f + f^2 d + b^2 f + c^2 d) \geq -4 \frac{128 + 8\pi^2}{\pi^3} \nu. \tag{6.14}$$

Putting inequalities (6.13) and (6.14) together we get

$$\begin{aligned} 8df - 4\nu(d^2 f + f^2 d + b^2 f + c^2 d) &\geq \frac{128}{\pi^2} s_\xi^2 s_\eta^2 (1 - \nu) - 4 \left(\frac{128 + 8\pi^2}{\pi^3} \right) \nu \\ &= \frac{128}{\pi^2} s_\xi^2 s_\eta^2 - \nu \left(\frac{128}{\pi^2} s_\xi^2 s_\eta^2 + 4 \left(\frac{128 + 8\pi^2}{\pi^3} \right) \right) \geq 0. \end{aligned}$$

The last inequality implies

$$\nu \leq \frac{\frac{128}{\pi^2} s_\xi^2 s_\eta^2}{4 \left(\frac{128 + 8\pi^2}{\pi^3} \right) + \frac{128}{\pi^2} s_\xi^2 s_\eta^2} \leq \frac{\frac{128}{\pi^2}}{4 \left(\frac{128 + 8\pi^2}{\pi^3} \right) + \frac{128}{\pi^2} s_\xi^2 s_\eta^2}.$$

Since

$$4 \left(\frac{128 + 8\pi^2}{\pi^3} \right) + \frac{128}{\pi^2} s_\xi^2 s_\eta^2 \geq 4 \left(\frac{128 + 8\pi^2}{\pi^3} \right)$$

we then have

$$\frac{1}{4 \left(\frac{128 + 8\pi^2}{\pi^3} \right) + \frac{128}{\pi^2} s_\xi^2 s_\eta^2} \leq \frac{1}{4 \left(\frac{128 + 8\pi^2}{\pi^3} \right)}.$$

Therefore we get

$$\nu \leq \frac{\frac{128}{\pi^2}}{\frac{4(128 + 8\pi^2)}{\pi^3}} = \frac{32\pi}{128 + 8\pi^2} \approx 0.4858. \tag{6.15}$$

Thus we have obtained a sufficient condition on ν for $\Delta^2 \geq 0$. For $\nu \leq 0.4858$ we have $\Delta^2 \geq 4(d^2 + f^2) \geq 0$.

Now $\Delta = 0$ corresponds to $d^2 + f^2 = 0$, which implies that $\lambda_r = 0$, cf. (6.8). Since we assume $\lambda_r > 0$ then $p(\lambda_r)$ has two distinct real roots r_1 and r_2, where

$$r_1 = (d+f) - \frac{\Delta}{2}, \qquad r_2 = (d+f) + \frac{\Delta}{2}.$$

Inequality (6.8) gives $\lambda_r \leq r_2$. To show that $\lambda_r \geq r_1$ note that from $\Delta \geq 4(d^2 + f^2)$ we have $r_1 \leq (d+f) - \sqrt{d^2+f^2}$. Furthermore $\sqrt{d^2+f^2} \geq \max(d, f)$. Therefore

$$r_1 \leq (d+f) - \sqrt{d^2+f^2} \leq (d+f) - \max(d,f) = \min(d,f) \leq \lambda_r.$$

Hence $\lambda_r \in [r_1, r_2]$. This implies that $p(\lambda_r) \leq 0$, what we wanted to show, cf. (6.12).
Now consider the case $\lambda_r = 0$, then either $d = 0$ or $f = 0$. Suppose $d = \frac{2}{\pi} s_\xi^2 (2 - \nu s_\eta^2) = 0$ then $s_\xi = 0$ and

$$\mathcal{D} + \mathcal{C} = \begin{pmatrix} \frac{4}{\pi} s_\eta^2 & 0 & S_\eta \\ 0 & 0 & 0 \\ -S_\eta & 0 & \frac{4}{\pi} s_\eta^2 \end{pmatrix}.$$

The eigenvalues of $\mathcal{D} + \mathcal{C}$ are 0, $\frac{4}{\pi} s_\eta^2 \pm i S_\eta$. Now $|\mu_c|^2 = |1 - \nu\lambda_c|^2 \leq 1$ gives

$$\begin{aligned} \left(1 - \nu\left(\frac{4}{\pi} s_\eta^2 + i S_\eta\right)\right)\left(1 - \nu\left(\frac{4}{\pi} s_\eta^2 - i S_\eta\right)\right) &= \left(\left(1 - \frac{4}{\pi}\nu s_\eta^2\right)^2 + \nu^2 S_\eta^2\right) \\ &= 1 - \frac{8\nu}{\pi} s_\eta^2 + \frac{16\nu^2}{\pi^2} s_\eta^4 + \nu^2 S_\eta^2 \leq 1. \end{aligned}$$

This leads to

$$-\frac{8\nu}{\pi} s_\eta^2 + \nu\left(\frac{16\nu}{\pi^2} s_\eta^4 + S_\eta^2\right) \leq 0.$$

Suppose $s_\eta \neq 0$, otherwise $\|\mathcal{H}\| = 1$ for any ν, then we have

$$\begin{aligned} -\frac{8}{\pi} + \nu\left(\frac{16}{\pi^2} + \left(\frac{S_\eta}{s_\eta}\right)^2\right) &\leq 0, \\ \nu\left(\frac{16}{\pi^2} + \left(\frac{S_\eta}{s_\eta}\right)^2\right) &\leq \frac{8}{\pi}. \end{aligned}$$

Now the last inequality yields

$$\nu \leq \frac{\frac{8}{\pi}}{\left(\frac{16}{\pi^2} + \left(\frac{S_\eta}{s_\eta}\right)^2\right)} \leq \frac{\pi}{2} \approx 1.5708. \tag{6.16}$$

Finally inequalities (6.10), (6.15) and (6.16) imply that if

$$\nu \leq \frac{32\pi}{128 + 8\pi^2} \approx 0.4858, \tag{6.17}$$

then the spectral radius of the matrix $\mathcal{H}$ is less than or equal to 1.

Remark 6.17 *It follows from the equation (6.6) that the error corresponding to the estimated stability limit of the scheme EG3*

$$0 \leq \nu \leq \frac{32\pi}{128 + 8\pi^2} \approx 0.4858$$

is less than or equal to $\frac{3}{8}\left(\frac{32\pi}{128+8\pi^2}\right)^2 \approx 0.0885$.

Hence we have proved the following result.

Lemma 6.18 *Consider the evolution Galerkin scheme EG3. Then, this scheme is stable if* $0 \leq \nu \leq \nu_{max} = \left(\frac{32\pi}{128+8\pi^2}\right) \approx 0.4858$. *The error corresponding to this estimation is less than or equal to* $\frac{3}{8}\left(\frac{32\pi}{128+8\pi^2}\right)^2 \approx 0.0885$.

Remark 6.19 *In the next table we have estimated the stability limit of the scheme EG3 using the standard MATLAB procedure for the eigenvalues of the matrix* $\mathcal{T}$. *Note that the upper bound of our theoretical result, i.e. 0.4858+0.0885=0.5743, matches very well with the experimental stability 0.58.*

$\frac{c\Delta t}{h}$	$\rho_{\xi,\eta}(\mathcal{T}(\xi,\eta))$ *for EG3*
0.10	1.000000000000000
0.20	1.000000000000000
0.30	1.000000000000000
0.40	1.000000000000000
0.50	1.000000000000000
0.58	1.000000000000000
0.59	1.000003244461521
0.60	1.000112236111448
0.70	1.008474049696319

Table 1: Stability limit using $\rho_{\xi,\eta}(\mathcal{T}(\xi,\eta))$.

In Figure 2 left we plot the eigenvalues of the matrix $\mathcal{H}$ as well as the unit circle. Similar plot with different scale is shown in Figure 2 right. With this simulation we illustrate that it is possible to include all eigenvalues, possibly except the eigenvalue 1, inside the unit circle. Since the entries of the of the matrix $\mathcal{H}$ are bounded, the condition stated in (6.17) is a necessary and sufficient stability condition, see Richtmyer and Morton [12]. In Figure 3 we show a sequence of plots, with different scales, of the eigenvalues of the amplification matrix corresponding to the first order EG3 scheme. Again using similar argument we conclude that the scheme is stable to CFL=0.58.

7 Approximate evolution operator E_Δ^{const} for piecewise constant data

In [2] Lukáčová, Morton and Warnecke proposed new approximate evolution operators E_Δ^{const} und E_Δ^{bilin} for the two-dimensional wave equation system and for the Euler equations of gas

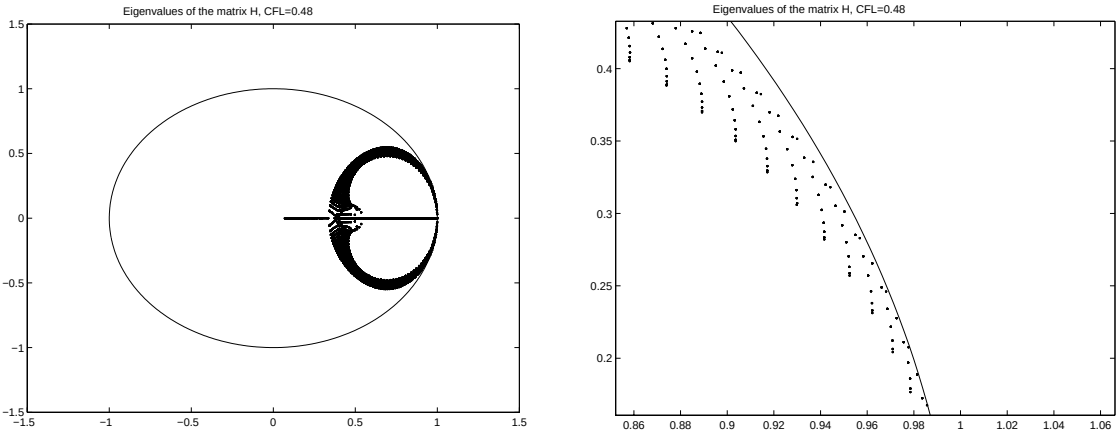

Figure 2: Eigenvalues of the matrix $\mathcal{H}$, CFL=0.48.

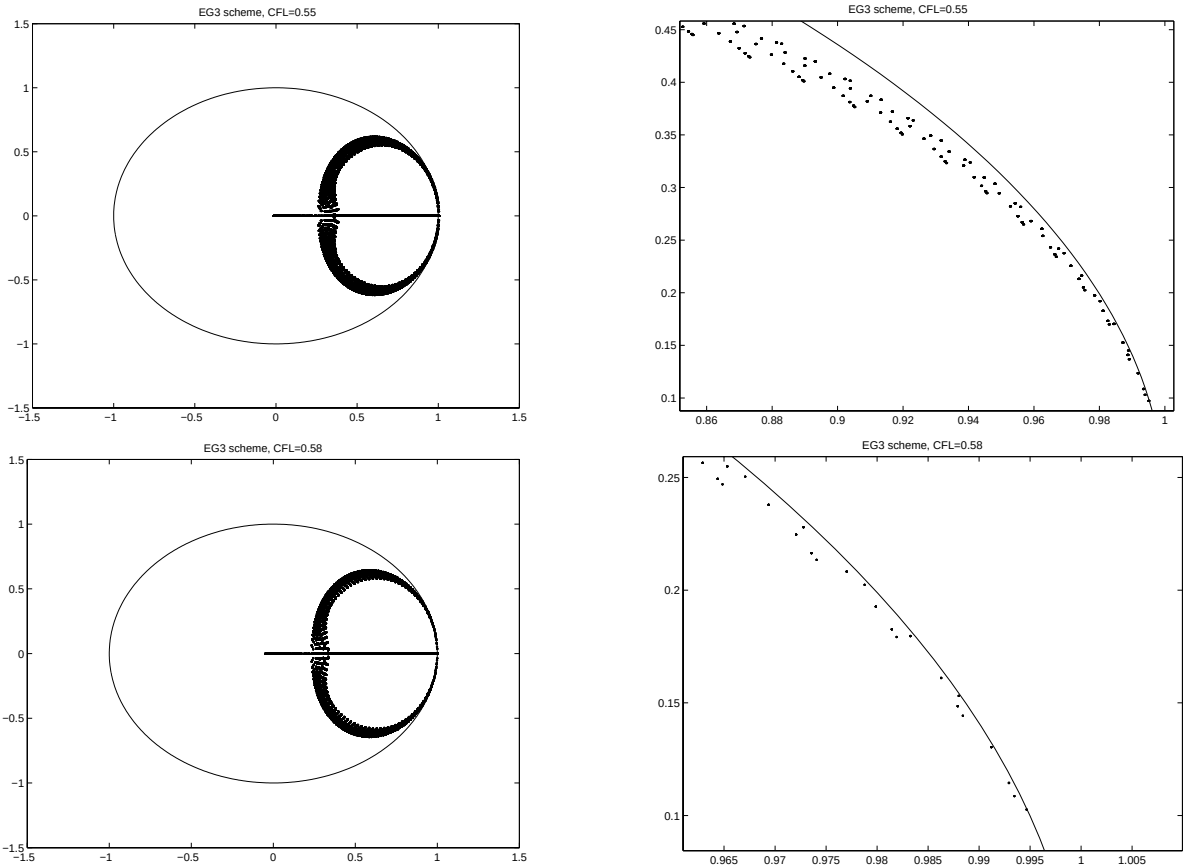

Figure 3: Eigenvalues of the amplification matrix of the first order EG3 scheme, CFL=0.55 (top), CFL=0.58 (bottom).

dynamics. Extensive numerical treatment presented in [2] indicates that these new operators improve the stability of the FVEG-schemes considerably. We will show that for special choices of discretization techniques stability limits close to the natural limit of 1 can be achieved. Numerical experiments, presented in [2], for these FVEG schemes confirm high accuracy as well as good multidimensional behaviour of new FVEG schemes. The key idea of the development of these new operators was to exploit the fact that the exact explicit solution to the one-dimensional wave equation system is available. Our new approximate operators are constructed in such a way that this exact solution is reproduced exactly for a given one-dimensional data. Thus, the approximate evolution operator E_Δ^{const} calculates exactly any one-dimensional wave, which is represented by a piecewise constant data and propagates either in $x-$ or $y-$ direction. Analogous situation holds for the operator E_Δ^{bilin} and approximated waves by means of continuous piecewise bilinear data. The approximate evolution operator E_Δ^{const} for piecewise constant data reads, cf. [2]

$$\begin{aligned}
\phi_P &= \frac{1}{2\pi}\int_0^{2\pi}(\phi_Q - u_Q \mathrm{sgn}\cos\theta - v_Q \mathrm{sgn}\sin\theta)\mathrm{d}\theta, && (7.1)\\
u_P &= \frac{1}{2\pi}\int_0^{2\pi}\left(-\phi_Q \mathrm{sgn}\cos\theta + u_Q\left(\frac{1}{2}+\cos^2\theta\right) + v_Q\sin\theta\cos\theta\right)\mathrm{d}\theta, && (7.2)\\
v_P &= \frac{1}{2\pi}\int_0^{2\pi}\left(-\phi_Q \mathrm{sgn}\sin\theta + u_Q\sin\theta\cos\theta + v_Q\left(\frac{1}{2}+\sin^2\theta\right)\right)\mathrm{d}\theta. && (7.3)
\end{aligned}$$

Integrations from 0 to 2π around the sonic circle in (7.1) - (7.3) are evaluated exactly. In this way all infinitely many directions of wave propagation are taken into account explicitly. For the cell interface integration along $\partial\Omega$ in (4.8) we have two possibilities. These edge integrals can either be computed exactly or numerically. Exact cell interface integration yields, e.g. for the vertical edge, the following intermediate values

$$\begin{aligned}
\tilde{\Phi}_{edge}^{n+\frac{1}{2}} &= \left(1+\frac{\nu}{2\pi}\delta_y^2\right)\mu_x\Phi^n - \left(\frac{1}{2}+\frac{\nu}{4\pi}\delta_y^2\right)\delta_x^2 U^n - \frac{\nu}{\pi}\mu_x\mu_y\delta_y V^n,\\
\tilde{U}_{edge}^{n+\frac{1}{2}} &= -\left(\frac{1}{2}+\frac{\nu}{4\pi}\delta_y^2\right)\delta_x\Phi^n + \left(1+\frac{5\nu}{12\pi}\delta_y^2\right)\mu_x^2 U^n + \frac{\nu}{6\pi}\delta_x\mu_y\delta_y V^n, && (7.4)
\end{aligned}$$

where $\mu_x f(x) = \frac{1}{2}\left(f\left(x+\frac{h}{2}\right)+f\left(x-\frac{h}{2}\right)\right)$, $\delta_x^2 f(x) = f(x+h)-2f(x)+f(x-h)$.
The stencil matrices of this FVEG scheme are given in the Appendix. Another possibility to evaluate the cell interface integrals is to use some numerical quadrature. In this way, further simplification in the evaluation of integrals can be made. Instead of the two-dimensional integrals along the cell interfaces and around the sonic circle, only the sonic circle integrals need to be evaluated exactly. In our experiments we used the trapezoidal rule and Simpson's rule for the cell interface integration. Thus, we need to determine $\tilde{\mathbf{U}}^{n+\frac{1}{2}}$

$$\begin{aligned}
\tilde{\Phi}_{vertex}^{n+\frac{1}{2}} &= \mu_x\mu_y\Phi^n - \frac{1}{2}\mu_y\delta_x U^n - \frac{1}{2}\mu_x\delta_y V^n,\\
\tilde{U}_{vertex}^{n+\frac{1}{2}} &= -\frac{1}{2}\mu_y\delta_x\Phi^n + \mu_x\mu_y U^n + \frac{1}{4\pi}\delta_x\delta_y V^n,\\
\tilde{\Phi}_{midpoint}^{n+\frac{1}{2}} &= \mu_x\Phi^n - \frac{1}{2}\delta_x U^n,\\
\tilde{U}_{midpoint}^{n+\frac{1}{2}} &= -\frac{1}{2}\delta_x\Phi^n + \mu_x U^n. && (7.5)
\end{aligned}$$

The stencil matrices of the FVEG scheme with the trapezoidal and the Simpson quadratures for the cell interface are given in the Appendix as well.
Analogous to the Section 6, we can show that the amplification matrix $\mathcal{T}$ of the first order FVEG scheme with exact edge integrals is similar to the matrix

$$\mathcal{Q} = \mathcal{I} - \nu\left(\mathcal{D} + \mathcal{C}\right) + \nu^2\tilde{\mathcal{C}},$$

where the matrix $\mathcal{D}$ is defined as before with

$$d = 2s_\xi^2\left(1 - \frac{2\nu}{\pi}s_\eta^2\right), \qquad f = 2s_\eta^2\left(1 - \frac{2\nu}{\pi}s_\xi^2\right).$$

The matrices $\mathcal{C}$ and $\tilde{\mathcal{C}}$ are given as

$$\mathcal{C} = \begin{pmatrix} 0 & C_\xi & C_\eta \\ C_\xi & 0 & 0 \\ C_\eta & 0 & 0 \end{pmatrix}, \qquad \tilde{\mathcal{C}} = \begin{pmatrix} 0 & \frac{1}{\pi}S_\xi & \frac{1}{\pi}S_\xi \\ 0 & 0 & C_{\xi\eta} \\ 0 & C_{\xi\eta} & 0 \end{pmatrix},$$

where

$$C_\xi = S_\xi\left(1 - \frac{2\nu}{\pi}s_\eta^2\right), \qquad C_\eta = S_\eta\left(1 - \frac{2\nu}{\pi}s_\xi^2\right),$$
$$C_{\xi\eta} = \frac{-1}{\pi}S_\xi S_\eta.$$

Since the matrix $\mathcal{C}$ is symmetric it is now not possible to carry out the analysis similar to the Section 6 in order to estimate the stability limit. Instead we use a MATLAB procedure to estimate the stability limit. The results are given in Table 2. In Column 2 we present the stability limit of the first order FVEG scheme with exact edge integrals. The stability limit of this scheme is improved considerably, the scheme is stable approximately up to the CFL=0.89. Column 3 demonstrates that the first order scheme based on the trapezoidal rule is stable to the natural stability limit 1. Column 4 shows that the stability of the first order scheme based on Simpson's rule is also increased, the scheme is stable approximately up to the CFL=0.75.

$\frac{c\Delta t}{h}$	Exact	Trapezoidal	Simpson
0.70	1.0000000000	1.0000000000	1.0000000000
0.75	1.0000000000	1.0000000000	1.0000000000
0.76	1.0000000000	1.0000000000	1.0206666667
0.80	1.0000000000	1.0000000000	
0.89	1.0000000000	1.0000000000	
0.90	1.0007993640	1.0000000000	
1.00		1.0000000000	
1.01		1.0200000000	

Table 2: Stability limit using $\rho_{\xi,\eta}(\mathcal{T}(\xi,\eta))$

In Figures 4 and 5 we plot, using different scales, the eigenvalues of the amplification matrices corresponding to the first order FVEG schemes based on the operator (7.1) - (7.3).

In Figure 4 top we used the exact integration along cell interfaces. In Figure 4 middle and bottom the trapezoidal rule was used to approximate the interface integrals. Analogous to the previous section, it is possible to encircle all eigenvalues, with exception of 1, in the unit circle. Since the entries of the amplification matrices are bounded the estimated stability limits are necessary conditions and sufficient as well. In Figure 5 we have plotted eigenvalues of the amplification matrix of the FVEG3 scheme with Simpson's rule approximation of the cell interface integrations.

8 Approximate evolution operator E_Δ^{bilin} for piecewise bilinear data

In this section we investigate the stability of the second order finite volume schemes proposed by Lukáčová *et al.* in [2]. These schemes are based on the approximate evolution operator E_Δ^{bilin}, which is given as

$$\begin{aligned}
\phi_P &= \left(1-\frac{\pi}{2}\right)\phi'_P + \frac{1}{2\pi}\int_0^{2\pi}\left(\frac{\pi}{2}\phi_Q - 2\cos\theta u_Q - 2\sin\theta v_Q\right)\mathrm{d}\theta + O(\Delta t^2), && (8.1)\\
u_P &= \left(1-\frac{\pi}{4}\right)u'_P + \frac{1}{2\pi}\int_0^{2\pi}\left(-2\cos\theta\phi_Q + \frac{\pi}{2}\left(3\cos^2\theta-1\right)u_Q + \frac{3\pi}{2}\sin\theta\cos\theta v_Q\right)\mathrm{d}\theta && (8.2)\\
&\qquad +O(\Delta t^2),\\
v_P &= \left(1-\frac{\pi}{4}\right)v'_P + \frac{1}{2\pi}\int_0^{2\pi}\left(-2\sin\theta\phi_Q + \frac{3\pi}{2}\sin\theta\cos\theta u_Q + \frac{\pi}{2}\left(3\sin^2\theta-1\right)v_Q\right)\mathrm{d}\theta && (8.3)\\
&\qquad +O(\Delta t^2).
\end{aligned}$$

Analogous to E_Δ^{const}, this approximate evolution operator is designed such that it computes any one-dimensional linear plane wave propagating in $x-$ or $y-$ direction exactly, for more details see [2]. In order to obtain second order finite volume schemes we carry out a recovery stage before applying the approximate evolution operator, see Definition 4.6. The following two types of bilinear recoveries have been considered in [2]

$$\begin{aligned}
R_h^C\mathbf{U}\big|_{\Omega_{kl}} &= \left(\mu_x^2\mu_y^2 + \frac{x-x_k}{h}\mu_x\mu_y^2\delta_x + \frac{y-y_l}{h}\mu_x^2\mu_y\delta_y + \frac{(x-x_k)(y-y_l)}{h}\mu_x\mu_y\delta_x\delta_y\right)\mathbf{U}_{kl}, && (8.4)\\
R_h^D\mathbf{U}\big|_{\Omega_{kl}} &= \left(1 + \frac{x-x_k}{h}\mu_x\mu_y^2\delta_x + \frac{y-y_l}{h}\mu_x^2\mu_y\delta_y + \frac{(x-x_k)(y-y_l)}{h}\mu_x\mu_y\delta_x\delta_y\right)\mathbf{U}_{kl}. && (8.5)
\end{aligned}$$

Note, that the recovery (8.4) is continuous while the recovery (8.5) is discontinuous and conservative. We use the midpoint rule to approximate the time integral in the equation (4.7). Denoting the cell interface intermediate value, that is computed in the predictor step (4.8), by $\mathbf{U}^{n+\frac{1}{2}}$ we can obtain the following schemes

$$\begin{aligned}
\text{scheme A} \qquad \mathbf{U}^{n+\frac{1}{2}} &= E_\Delta^{bilin}R_h^C\mathbf{U}^n + E_\Delta^{const}(1-\mu_x^2\mu_y^2)\mathbf{U}^n,\\
\text{scheme B} \qquad \mathbf{U}^{n+\frac{1}{2}} &= E_\Delta^{bilin}R_h^C\mathbf{U}^n,\\
\text{scheme C} \qquad \mathbf{U}^{n+\frac{1}{2}} &= E_\Delta^{bilin}R_h^D\mathbf{U}^n.
\end{aligned}$$

Each of these schemes has further two types according to the evaluation of the cell interface integrals. We used the subscripts 1, 2 to distinguish between them. Thus, 1 corresponds to

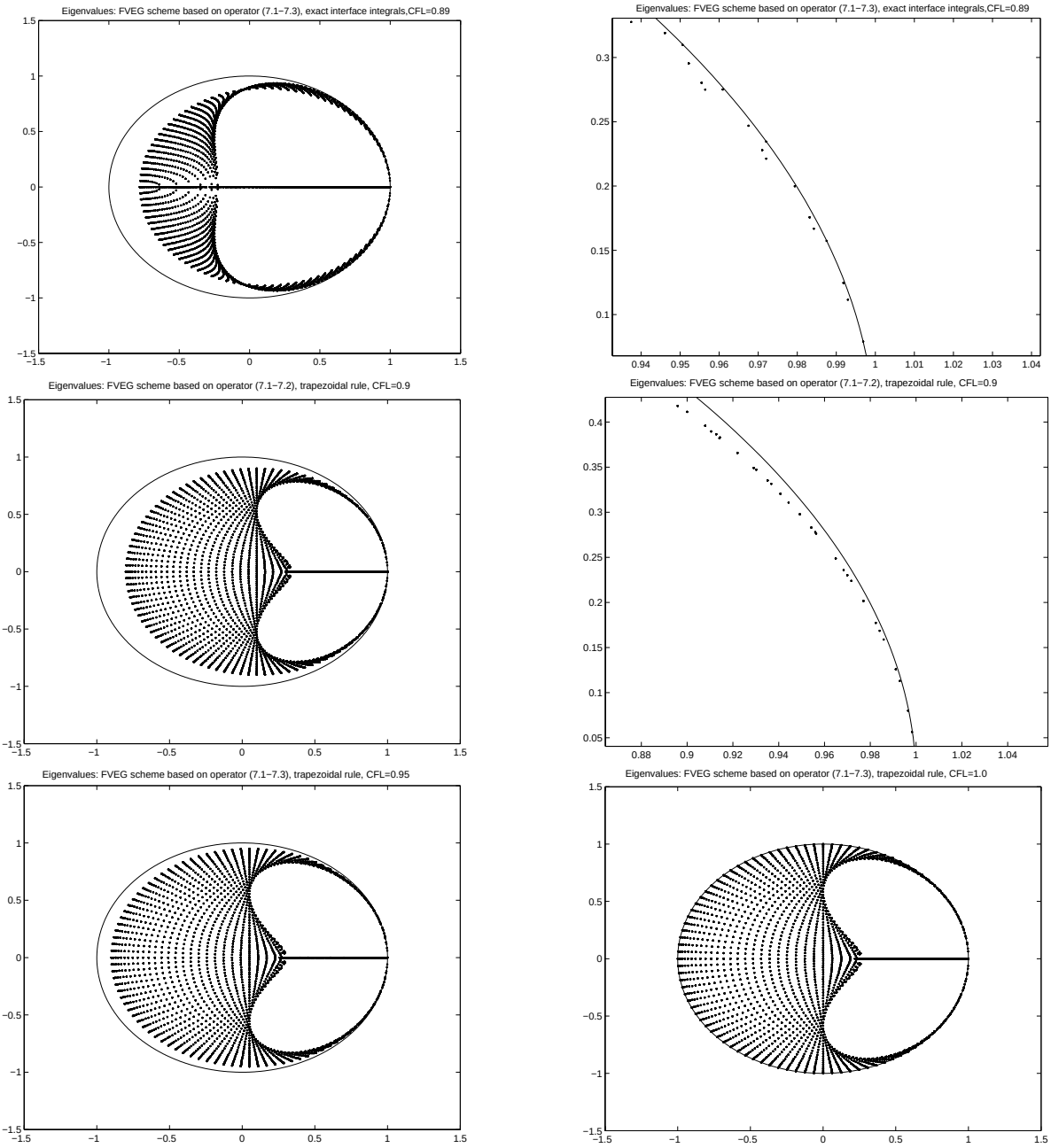

Figure 4: Eigenvalues of the amplification matrices: top: exact interface integration (CFL=0.89), middle and bottom: interface integrals approximated using the trapezoidal rule for the CFL=0.9, 0.95, 1.0.

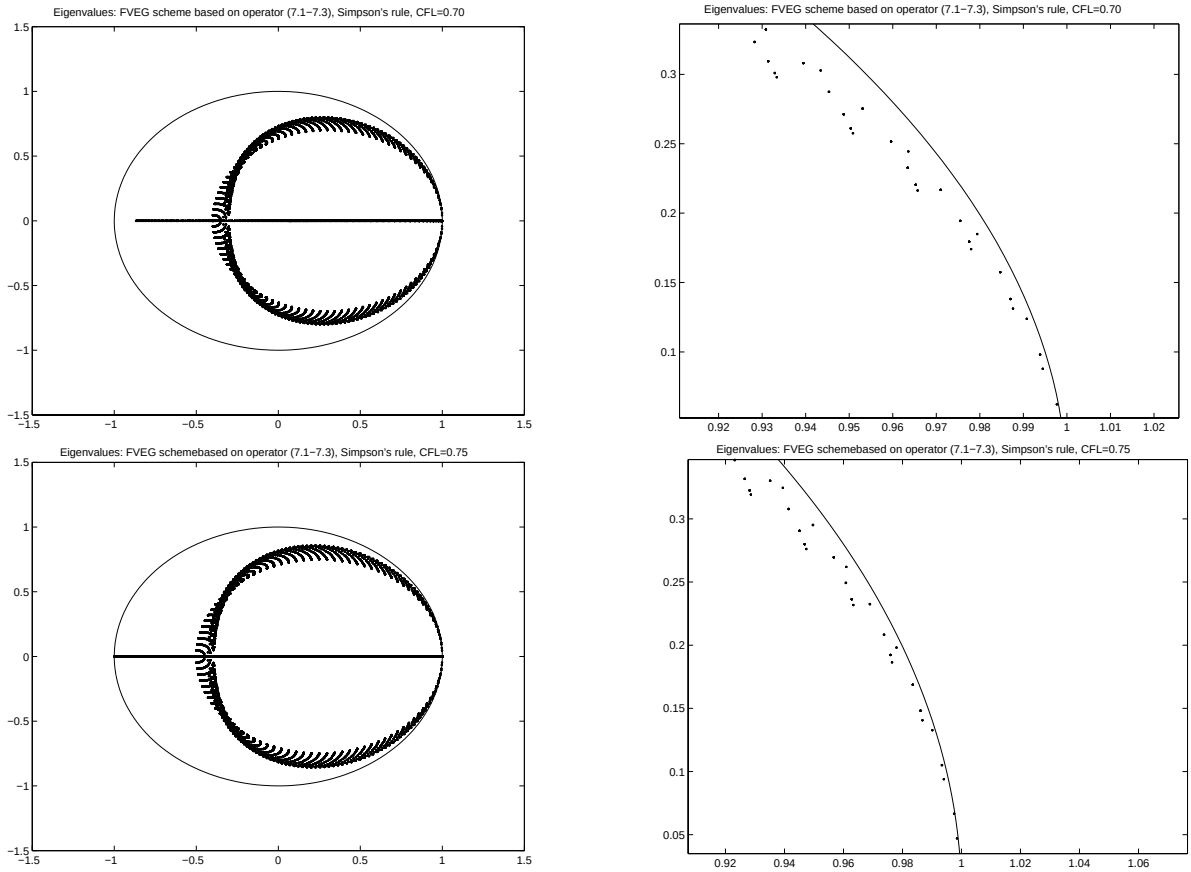

Figure 5: Eigenvalues of the amplification matrix, interface integrals approximated using Simpson's rule, CFL=0.7 (top), CFL=0.75 (bottom).

Simpson's rule and 2 for the trapezoidal rule. For example, for the scheme C_2 the predicted values along the right cell interface are

$$\begin{aligned}
\tilde{\Phi}^{n+\frac{1}{2}} &= \left[1+\left(\frac{-\pi}{32}+\frac{\nu}{16}\right)\delta_x^2\mu_y^2+\left(\frac{-\pi}{32}+\frac{\nu}{16}\right)\delta_y^2\mu_x^2+\left(\frac{\pi}{32}-\frac{\nu}{8}+\frac{\nu^2}{32}\right)\delta_x^2\delta_y^2\right]\mu_x\mu_y\Phi^n \\
&+\left[\frac{-2}{\pi}+\left(\frac{1}{2\pi}-\frac{\nu}{8}\right)\mu_x^2\mu_y^2+\left(\frac{1}{8\pi}-\frac{\nu}{16\pi}\right)\delta_y^2\mu_x^2+\left(\frac{-1}{2\pi}+\frac{\nu}{8}+\frac{\nu}{4\pi}-\frac{\nu^2}{6\pi}\right)\mu_x^2\delta_y^2\right]\delta_x\mu_y U^n \\
&+\left[\frac{-2}{\pi}+\left(\frac{1}{8\pi}-\frac{\nu}{16\pi}\right)\delta_x^2\mu_y^2+\left(\frac{1}{2\pi}-\frac{\nu}{8}\right)\mu_x^2\mu_y^2+\left(\frac{-1}{2\pi}+\frac{\nu}{8}+\frac{\nu}{4\pi}-\frac{\nu^2}{6\pi}\right)\mu_y^2\delta_x^2\right]\delta_y\mu_x V^n
\end{aligned}$$

$$\begin{aligned}
\tilde{U}^{n+\frac{1}{2}} &= \left[\frac{-2}{\pi}+\left(\frac{1}{2\pi}-\frac{\nu}{8}\right)\mu_x^2\mu_y^2+\left(\frac{1}{8\pi}-\frac{\nu}{16\pi}\right)\delta_y^2\mu_x^2+\right. \\
&\qquad\left.\left(\frac{-1}{2\pi}+\frac{\nu}{8}+\frac{\nu}{4\pi}-\frac{\nu^2}{6\pi}\right)\mu_x^2\delta_y^2\right]\delta_x\mu_y\Phi^n \\
&+\left[1+\left(\frac{-\pi}{64}+\frac{\nu}{16}\right)\delta_x^2\mu_y^2-\frac{\pi}{64}\delta_y^2\mu_x^2+\left(\frac{\pi}{64}-\frac{\nu}{16}+\frac{\nu^2}{64}\right)\delta_x^2\delta_y^2\right]\mu_x\mu_y U^n \\
&+\left[\frac{1}{8}+\left(\frac{1}{16}-\frac{\nu}{8}+\frac{\pi\nu^2}{64}\right)\mu_x^2\mu_y^2\right]3\delta_x\delta_y V^n
\end{aligned}$$

with the equation for $\tilde{V}^{n+\frac{1}{2}}$ that is analogous to that of $\tilde{U}^{n+\frac{1}{2}}$. Further, we can express analogously the predicted values for other cell interfaces as well as for other schemes. Substituting the predicted values in the corrector step (4.7) yields for all second order finite volume schemes FVEG-A, B, C

$$\mathbf{U}_{kl}^{n+1} = \mathbf{U}_{kl}^n+\sum_{r=-1}^{1}\sum_{s=-1}^{1}\mathcal{C}_{rs}\mathbf{U}_{k+rl+s}^n+\mathcal{C}_{rs}^x\mathbf{U}_{x_{k+rl+s}}^n+\mathcal{C}_{rs}^y\mathbf{U}_{y_{k+rl+s}}^n+\mathcal{C}_{rs}^{xy}\mathbf{U}_{xy_{k+rl+s}}^n, \tag{8.6}$$

where $\mathcal{C}_{rs}^x$, $\mathcal{C}_{rs}^y$ and $\mathcal{C}_{rs}^{xy}$ are the coefficient matrices corresponding to the approximation of $x-$, $y-$, and $xy-$ slopes. Moreover,

$$\mathbf{U}_{x_{k+rl+s}}^n=\mu_x\mu_y^2\delta_x\mathbf{U}_{k+rl+s}^n,\ \mathbf{U}_{y_{k+rl+s}}^n=\mu_x^2\mu_y\delta_y\mathbf{U}_{k+rl+s}^n,\ \mathbf{U}_{xy_{k+rl+s}}^n=\mu_x\mu_y\delta_x\delta_y\mathbf{U}_{k+rl+s}^n.$$

Applying the von Neumann analysis and the Fourier transformation we derive the amplification matrices $\mathcal{T}$. It should be pointed out that their structure is too complicated in order to apply the similar estimates of the spectral radius as we did in Section 6 for the first order EG3 scheme. Anyway, we can use the standard MATLAB procedure to determine the eigenvalues of $\mathcal{T}$. This yields the stability limits given in Table 3.

In Figures 6 and 7 we plot, using different scales, the eigenvalues of the amplification matrices corresponding to the second order FVEG schemes; scheme A_i, B_i and C_i, where $i=1,2$. Similar to the previous cases, these plots indicate that all eigenvalues, possibly except of 1, can be bounded inside the unit circle. Thus the stability limits which we obtained are necessary as well as sufficient conditions.

Further, it follows from Figure 6 that the second order FVEG scheme based on the operator (8.1) - (8.3) with the continuous non-conservative recovery (8.4) using Simpson's rule to approximate the cell interface integrals, i.e. scheme B_1, is unconditionally unstable. This

	Trapezoidal rule	Simpson's rule
scheme A	0.94	0.75
scheme B	0.78	-
scheme C	0.78	0.58

Table 3: Stability limits of the second order FVEG schemes.

fact has also been confirmed by other numerical tests for the wave equation system with discontinuous solution, see the Problem 3 in [4]. We have found for all CFL numbers, no matter how small they were chosen, instabilities in the solution for fine enough meshes. We should note that all other CFL limits given in the Table 3 have also been confirmed by particular numerical experiments.

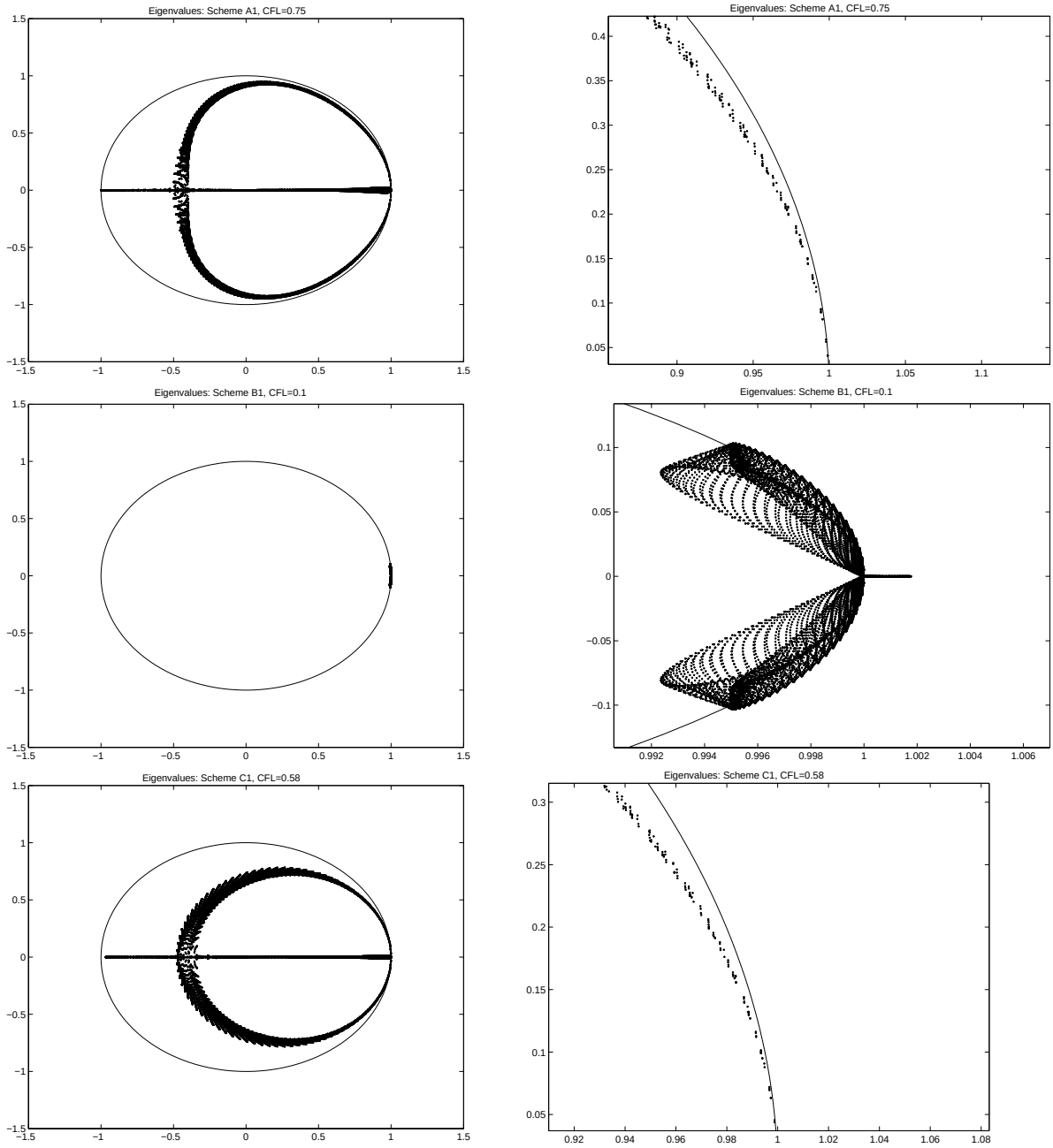

Figure 6: Eigenvalues corresponding to the amplification matrices of the scheme A_1 (CFL=0.75), scheme B_1 (CFL=0.1), and the scheme C_1 (CFL=0.58).

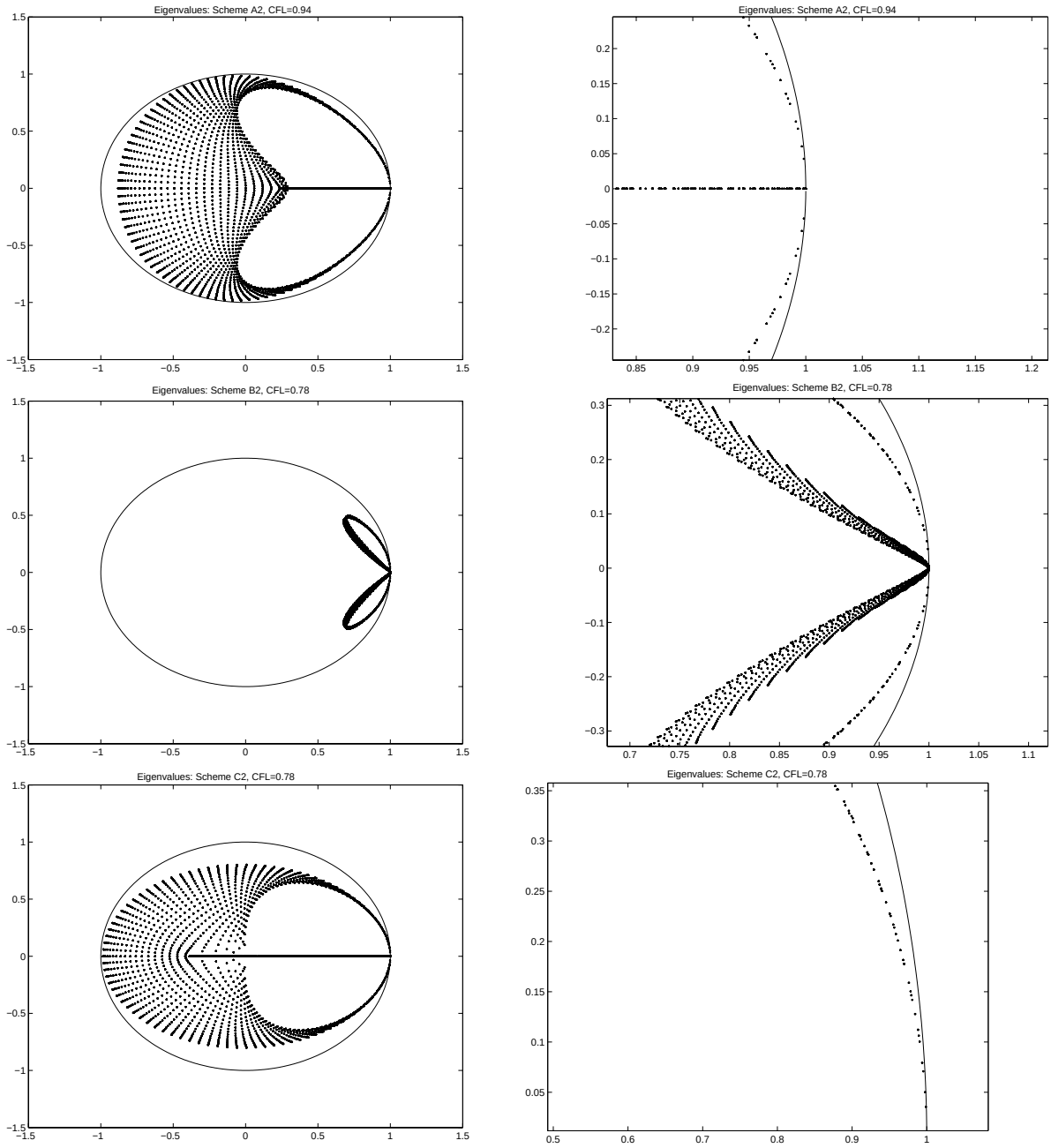

Figure 7: Eigenvalues corresponding to the amplification matrices of the scheme A_2 (CFL=0.94), scheme B_2 (CFL=0.78), scheme C_2 (CFL=0.78).

Appendix

EG3 scheme

$$\alpha^1 := \left\{ \begin{array}{ccc} \frac{\nu^2}{4\pi} & \frac{\nu}{\pi} - \frac{\nu^2}{2\pi} & \frac{\nu^2}{4\pi} \\ \frac{\nu}{\pi} - \frac{\nu^2}{2\pi} & -\frac{4\nu}{\pi} + \frac{\nu^2}{\pi} & \frac{\nu}{\pi} - \frac{\nu^2}{2\pi} \\ \frac{\nu^2}{4\pi} & \frac{\nu}{\pi} - \frac{\nu^2}{2\pi} & \frac{\nu^2}{4\pi} \end{array} \right\}, \quad \beta^1 := \left\{ \begin{array}{ccc} \frac{\nu^2}{3\pi} & 0 & \frac{-\nu^2}{3\pi} \\ \frac{\nu}{2} - \frac{2\nu^2}{3\pi} & 0 & -\frac{\nu}{2} + \frac{2\nu^2}{3\pi} \\ \frac{\nu^2}{3\pi} & 0 & -\frac{\nu^2}{3\pi} \end{array} \right\},$$

$$\gamma^1 := \left\{ \begin{array}{ccc} -\frac{\nu^2}{3\pi} & -\frac{\nu}{2} + \frac{2\nu^2}{3\pi} & -\frac{\nu^2}{3\pi} \\ 0 & 0 & 0 \\ \frac{\nu^2}{3\pi} & \frac{\nu}{2} - \frac{2\nu^2}{3\pi} & \frac{\nu^2}{3\pi} \end{array} \right\}, \quad \alpha^2 := \left\{ \begin{array}{ccc} \frac{\nu^2}{3\pi} & 0 & -\frac{\nu^2}{3\pi} \\ \frac{\nu}{2} - \frac{2\nu^2}{3\pi} & 0 & -\frac{\nu}{2} + \frac{2\nu^2}{3\pi} \\ \frac{\nu^2}{3\pi} & 0 & \frac{-\nu^2}{3\pi} \end{array} \right\},$$

$$\beta^2 := \left\{ \begin{array}{ccc} \frac{\nu^2}{8\pi} & -\frac{\nu^2}{4\pi} & \frac{\nu^2}{8\pi} \\ \frac{\nu}{\pi} - \frac{\nu^2}{4\pi} & -\frac{2\nu}{\pi} + \frac{\nu^2}{2\pi} & \frac{\nu}{\pi} - \frac{\nu^2}{4\pi} \\ \frac{\nu^2}{8\pi} & -\frac{\nu^2}{4\pi} & \frac{\nu^2}{8\pi} \end{array} \right\}, \quad \gamma^2 := \left\{ \begin{array}{ccc} -\frac{3\nu^2}{32} & 0 & \frac{3\nu^2}{32} \\ 0 & 0 & 0 \\ \frac{3\nu^2}{32} & 0 & -\frac{3\nu^2}{32} \end{array} \right\},$$

$$\alpha^3 := \left\{ \begin{array}{ccc} -\frac{\nu^2}{3\pi} & -\frac{\nu}{2} + \frac{2\nu^2}{3\pi} & -\frac{\nu^2}{3\pi} \\ 0 & 0 & 0 \\ \frac{\nu^2}{3\pi} & +\frac{\nu}{2} - \frac{2\nu^2}{3\pi} & \frac{\nu^2}{3\pi} \end{array} \right\}, \quad \beta^3 := \left\{ \begin{array}{ccc} -\frac{3\nu^2}{32} & 0 & \frac{3\nu^2}{32} \\ 0 & 0 & 0 \\ \frac{3\nu^2}{32} & 0 & -\frac{3\nu^2}{32} \end{array} \right\},$$

$$\gamma^3 := \left\{ \begin{array}{ccc} \frac{\nu^2}{8\pi} & \frac{\nu}{\pi} - \frac{\nu^2}{4\pi} & \frac{\nu^2}{8\pi} \\ -\frac{\nu^2}{4\pi} & -\frac{2\nu}{\pi} + \frac{\nu^2}{2\pi} & -\frac{\nu^2}{4\pi} \\ \frac{\nu^2}{8\pi} & \frac{\nu}{\pi} - \frac{\nu^2}{4\pi} & \frac{\nu^2}{8\pi} \end{array} \right\}.$$

FVEG scheme based on operator E_{Δ}^{const} with exact cell inteface integrals

$$\alpha^1 := \left\{ \begin{array}{ccc} \frac{\nu^2}{2\pi} & \frac{\nu}{2} - \frac{\nu^2}{\pi} & \frac{\nu^2}{2\pi} \\ \frac{\nu}{2} - \frac{\nu^2}{\pi} & -2\nu + \frac{2\nu^2}{\pi} & \frac{\nu}{2} - \frac{\nu^2}{\pi} \\ \frac{\nu^2}{2\pi} & \frac{\nu}{2} - \frac{\nu^2}{\pi} & \frac{\nu^2}{2\pi} \end{array} \right\}, \quad \beta^1 := \left\{ \begin{array}{ccc} \frac{7\nu^2}{24\pi} & 0 & \frac{-7\nu^2}{24\pi} \\ \frac{\nu}{2} - \frac{7\nu^2}{12\pi} & 0 & \frac{-\nu}{2} + \frac{7\nu^2}{12\pi} \\ \frac{7\nu^2}{24\pi} & 0 & \frac{-7\nu^2}{24\pi} \end{array} \right\},$$

$$\gamma^1 := \left\{ \begin{array}{ccc} \frac{-7\nu^2}{24\pi} & \frac{-\nu}{2} + \frac{7\nu^2}{12\pi} & \frac{-7\nu^2}{24\pi} \\ 0 & 0 & 0 \\ \frac{7\nu^2}{24\pi} & \frac{\nu}{2} - \frac{7\nu^2}{12\pi} & \frac{7\nu^2}{24\pi} \end{array} \right\}, \quad \alpha^2 := \left\{ \begin{array}{ccc} \frac{\nu^2}{4\pi} & 0 & \frac{-\nu^2}{4\pi} \\ \frac{\nu}{2} - \frac{\nu^2}{2\pi} & 0 & \frac{-\nu}{2} + \frac{\nu^2}{2\pi} \\ \frac{\nu^2}{4\pi} & 0 & \frac{-\nu^2}{4\pi} \end{array} \right\},$$

$$\beta^2 := \left\{ \begin{array}{ccc} \frac{\nu^2}{4\pi} & -\frac{\nu^2}{2\pi} & \frac{\nu^2}{4\pi} \\ \frac{\nu}{2} - \frac{\nu^2}{2\pi} & -\nu + \frac{\nu^2}{\pi} & \frac{\nu}{2} - \frac{\nu^2}{2\pi} \\ \frac{\nu^2}{4\pi} & -\frac{\nu^2}{2\pi} & \frac{\nu^2}{4\pi} \end{array} \right\}, \quad \gamma^2 := \left\{ \begin{array}{ccc} \frac{-\nu^2}{4\pi} & 0 & \frac{\nu^2}{4\pi} \\ 0 & 0 & 0 \\ \frac{\nu^2}{4\pi} & 0 & \frac{-\nu^2}{4\pi} \end{array} \right\},$$

$$\alpha^3 := \left\{ \begin{array}{ccc} \frac{-\nu^2}{4\pi} & \frac{-\nu}{2} + \frac{\nu^2}{2\pi} & \frac{-\nu^2}{4\pi} \\ 0 & 0 & 0 \\ \frac{\nu^2}{4\pi} & \frac{\nu}{2} - \frac{\nu^2}{2\pi} & \frac{\nu^2}{4\pi} \end{array} \right\}, \quad \beta^3 := \left\{ \begin{array}{ccc} \frac{-\nu^2}{4\pi} & 0 & \frac{\nu^2}{4\pi} \\ 0 & 0 & 0 \\ \frac{\nu^2}{4\pi} & 0 & \frac{-\nu^2}{4\pi} \end{array} \right\},$$

$$\gamma^3 := \left\{ \begin{array}{ccc} \frac{\nu^2}{4\pi} & \frac{\nu}{2} - \frac{\nu^2}{2\pi} & \frac{\nu^2}{4\pi} \\ -\frac{\nu^2}{2\pi} & -\nu + \frac{\nu^2}{\pi} & -\frac{\nu^2}{2\pi} \\ \frac{\nu^2}{4\pi} & \frac{\nu}{2} - \frac{\nu^2}{2\pi} & \frac{\nu^2}{4\pi} \end{array} \right\}.$$

FVEG with E_{Δ}^{const} operator using Simpson's quadrature for cell interface integration

$$\alpha^1 := \left\{ \begin{array}{ccc} \frac{\nu}{12} & \frac{\nu}{3} & \frac{\nu}{12} \\ \frac{\nu}{3} & -\frac{5\nu}{3} & \frac{\nu}{3} \\ \frac{\nu}{12} & \frac{\nu}{3} & \frac{\nu}{12} \end{array} \right\}, \quad \beta^1 := \left\{ \begin{array}{ccc} \frac{\nu}{24}\left(1+\frac{1}{\pi}\right) & 0 & -\frac{\nu}{24}\left(1+\frac{1}{\pi}\right) \\ \frac{\nu}{24}\left(10-\frac{2}{\pi}\right) & 0 & -\frac{\nu}{24}\left(10-\frac{2}{\pi}\right) \\ \frac{\nu}{24}\left(1+\frac{1}{\pi}\right) & 0 & -\frac{\nu}{24}\left(1+\frac{1}{\pi}\right) \end{array} \right\},$$

$$\gamma^1 := \left\{ \begin{array}{ccc} -\frac{\nu}{24}\left(1+\frac{1}{\pi}\right) & -\frac{\nu}{24}\left(10-\frac{2}{\pi}\right) & -\frac{\nu}{24}\left(1+\frac{1}{\pi}\right) \\ 0 & 0 & 0 \\ \frac{\nu}{24}\left(1+\frac{1}{\pi}\right) & \frac{\nu}{24}\left(10-\frac{2}{\pi}\right) & \frac{\nu}{24}\left(1+\frac{1}{\pi}\right) \end{array} \right\}, \quad \alpha^2 := \left\{ \begin{array}{ccc} \frac{\nu}{24} & 0 & -\frac{\nu}{24} \\ \frac{10\nu}{24} & 0 & -\frac{10\nu}{24} \\ \frac{\nu}{24} & 0 & -\frac{\nu}{24} \end{array} \right\},$$

$$\beta^2 := \left\{ \begin{array}{ccc} \frac{\nu}{24} & -\frac{2\nu}{24} & \frac{\nu}{24} \\ \frac{10\nu}{24} & -\frac{20\nu}{24} & \frac{10\nu}{24} \\ \frac{\nu}{24} & -\frac{2\nu}{24} & \frac{\nu}{24} \end{array} \right\}, \quad \gamma^2 := \left\{ \begin{array}{ccc} -\frac{\nu}{24} & 0 & \frac{\nu}{24} \\ 0 & 0 & 0 \\ \frac{\nu}{24} & 0 & -\frac{\nu}{24} \end{array} \right\},$$

$$\alpha^3 := \left\{ \begin{array}{ccc} -\frac{\nu}{24} & -\frac{10\nu}{24} & -\frac{\nu}{24} \\ 0 & 0 & 0 \\ \frac{\nu}{24} & \frac{10\nu}{24} & \frac{\nu}{24} \end{array} \right\}, \quad \beta^3 := \left\{ \begin{array}{ccc} -\frac{\nu}{24} & 0 & \frac{\nu}{24} \\ 0 & 0 & 0 \\ \frac{\nu}{24} & 0 & -\frac{\nu}{24} \end{array} \right\},$$

$$\gamma^3 := \left\{ \begin{array}{ccc} \frac{\nu}{24} & \frac{10\nu}{24} & \frac{\nu}{24} \\ -\frac{2\nu}{24} & -\frac{20\nu}{24} & -\frac{2\nu}{24} \\ \frac{\nu}{24} & \frac{10\nu}{24} & \frac{\nu}{24} \end{array} \right\}.$$

FVEG with E_{Δ}^{const} operator using the trapezoidal quadrature for cell interface integration

$$\alpha^1 := \left\{ \begin{array}{ccc} \frac{\nu}{4} & 0 & \frac{\nu}{4} \\ 0 & -\nu & 0 \\ \frac{\nu}{4} & 0 & \frac{\nu}{4} \end{array} \right\}, \quad \beta^1 := \left\{ \begin{array}{ccc} \frac{\nu}{8}\left(1+\frac{1}{\pi}\right) & 0 & -\frac{\nu}{8}\left(1+\frac{1}{\pi}\right) \\ \frac{\nu}{8}\left(2-\frac{2}{\pi}\right) & 0 & -\frac{\nu}{8}\left(2-\frac{2}{\pi}\right) \\ \frac{\nu}{8}\left(1+\frac{1}{\pi}\right) & 0 & -\frac{\nu}{8}\left(1+\frac{1}{\pi}\right) \end{array} \right\},$$

$$\gamma^1 := \left\{ \begin{array}{ccc} -\frac{\nu}{8}\left(1+\frac{1}{\pi}\right) & -\frac{\nu}{8}\left(2-\frac{2}{\pi}\right) & -\frac{\nu}{8}\left(1+\frac{1}{\pi}\right) \\ 0 & 0 & 0 \\ \frac{\nu}{8}\left(1+\frac{1}{\pi}\right) & \frac{\nu}{8}\left(2-\frac{2}{\pi}\right) & \frac{\nu}{8}\left(1+\frac{1}{\pi}\right) \end{array} \right\}, \quad \alpha^2 := \left\{ \begin{array}{ccc} \frac{\nu}{8} & 0 & -\frac{\nu}{8} \\ \frac{2\nu}{8} & 0 & -\frac{2\nu}{8} \\ \frac{\nu}{8} & 0 & -\frac{\nu}{8} \end{array} \right\},$$

$$\beta^2 := \left\{ \begin{array}{ccc} \frac{\nu}{8} & -\frac{2\nu}{8} & \frac{\nu}{8} \\ \frac{2\nu}{8} & -\frac{4\nu}{8} & \frac{2\nu}{8} \\ \frac{\nu}{8} & -\frac{2\nu}{8} & \frac{\nu}{8} \end{array} \right\}, \quad \gamma^2 := \left\{ \begin{array}{ccc} -\frac{\nu}{8} & 0 & \frac{\nu}{8} \\ 0 & 0 & 0 \\ \frac{\nu}{8} & 0 & -\frac{\nu}{8} \end{array} \right\},$$

$$\alpha^3 := \left\{ \begin{array}{ccc} -\frac{\nu}{8} & -\frac{2\nu}{8} & -\frac{\nu}{8} \\ 0 & 0 & 0 \\ \frac{\nu}{8} & \frac{2\nu}{8} & \frac{\nu}{8} \end{array} \right\}, \quad \beta^3 := \left\{ \begin{array}{ccc} -\frac{\nu}{8} & 0 & \frac{\nu}{8} \\ 0 & 0 & 0 \\ \frac{\nu}{8} & 0 & -\frac{\nu}{8} \end{array} \right\},$$

$$\gamma^3 := \left\{ \begin{array}{ccc} \frac{\nu}{8} & \frac{2\nu}{8} & \frac{\nu}{8} \\ -\frac{2\nu}{8} & -\frac{4\nu}{8} & -\frac{2\nu}{8} \\ \frac{\nu}{8} & \frac{2\nu}{8} & \frac{\nu}{8} \end{array} \right\}.$$

References

[1] M. Lukáčová, K. W. Morton, and G. Warnecke. Finite volume evolution Galerkin methods for Euler equations of gas dynamics. *Int. J. Num. Methods in Fluids*, 40(3-4):425–434, 2002.

[2] M. Lukáčová, K.W. Morton, and G. Warnecke. Finite volume evolution Galerkin (FVEG) methods for hyperbolic systems, accepted to *SISC*, 2003.

[3] M. Lukáčová, K.W. Morton, and G. Warnecke. High resolution finite volume evolution Galerkin schemes for multidimensional conservation laws. Proceedings of ENNUMA-MATH'99, World Scientific Publishing Company, Singapore, 1999.

[4] M. Lukáčová, K.W. Morton, and G. Warnecke. Evolution Galerkin methods for hyperbolic systems in two space dimensions. *Math. Comput.*, 69(232):1355–1384, 2000.

[5] M. Lukáčová, K.W. Morton, and G. Warnecke. Evolution Galerkin methods for multidimensional hyperbolic systems. Proceedings of ECCOMAS 2000, Barcelona, 1-14, 2000.

[6] M. Lukáčová, J. Saibertová, and G. Warnecke. Finite volume evolution Galerkin methods for nonlinear hyperbolic systems. *J. Comput. Phys.*, 183:533–562, 2002.

[7] M. Lukáčová, J. Saibertová, G. Warnecke, and Y. Zahaykah. On evolution Galerkin methods for the Maxwell and the linearized Euler equations, accepted to Appl. Math., 2003.

[8] M. Lukáčová, G. Warnecke, and Y. Zahaykah. Third order finite volume evolution Galerkin (FVEG) methods for two-dimensional wave equation system, *J. Numer. Math.*, 11(3):235-251, 2003.

[9] P. Lin, K.W. Morton, and E. Süli. Euler characteristic Galerkin scheme with recovery, M^2AN, 27(7):863–894, 1993.

[10] P. Lin, K.W. Morton, and E. Süli. Characteristic Galerkin schemes for scalar conservation laws in two and three space dimensions, *SIAM J. Numer. Anal.*, 34(2):779–796, 1997.

[11] S. Ostkamp. Multidimensional characteristic Galerkin schemes and evolution operators for hyperbolic systems. *Math. Meth. Appl. Sci.*, 20:1111–1125, 1997.

[12] R. D. Richtmyer and K. W. Morton. *Difference methods for initial-value problems.* Krieger Publishing Company, Malabar, Florida, 1994.

[13] Y. Zahaykah. *Evolution Galerkin Schemes and Discrete Boundary Conditions for Multidimensional First Order Systems.* Dissertation, Magdeburg, 2002.